Results in Engineering 28 (2025) 107583

Contents lists available at ScienceDirect

Results in Engineering

journal homepage: www.sciencedirect.com/journal/results-in-engineering

Review article

A narrative review on collateral circulation classification for ischemic stroke

Kazi Ashikur Rahman [a], Nur Hasanah Ali [b,*], Ahmad Sobri Muda [c]

[a] Faculty of Electrical Technology and Engineering, Universiti Teknikal Malaysia Melaka, Melaka, Malaysia
[b] Faculty of Engineering and Technology, Multimedia University, Melaka, Malaysia
[c] Neurovascular & Clinical Centre, Hospital Sultan Abdul Aziz Shah (HSAAS), Universiti Putra Malaysia, Malaysia

ARTICLE INFO

Keywords:
Collateral circulation
Brain stroke
Ischemic stroke
Deep learning
CNN
VGG11
ResNet-50

ABSTRACT

This review explores recent advancements in the classification of collateral circulation in ischemic stroke, with a focus on artificial intelligence-driven imaging analysis. It provides a comprehensive overview of stroke types, the physiological importance of collateral networks, and compares imaging modalities such as CT, MRI, and Cone Beam Computed Tomography (CBCT) for collateral assessment. The paper also examines various collateral scoring systems, highlighting both manual and automated methods. Particular attention is given to machine learning and deep learning classification techniques, including convolutional neural networks, residual networks, and multimodal fusion strategies aimed at improving diagnostic accuracy and reproducibility. Key challenges such as data variability, model generalizability, and explainability are discussed, along with future research directions to enhance clinical applicability. This review underscores the increasing role of AI-based classification in enabling faster, more accurate collateral evaluation and improving patient outcomes in ischemic stroke management.

Contents

* Corresponding author.
E-mail address: hasanah.ali@mmu.edu.my (N.H. Ali).

https://doi.org/10.1016/j.rineng.2025.107583
Received 21 May 2025; Received in revised form 22 September 2025; Accepted 4 October 2025

Available online 10 October 2025

1. Introduction

Ischemic stroke is one of the leading causes of death and long-term disability worldwide, accounting for over 80% of all stroke cases [1]. According to global estimates, more than 12 million people suffer a stroke each year, with a substantial proportion resulting in permanent neurological impairments [2]. This condition is primarily caused by the obstruction of a cerebral artery due to thrombosis or embolism, resulting in reduced blood flow and oxygen deprivation to critical brain tissues. Without timely medical intervention, irreversible neuronal damage can occur within minutes.

To mitigate the effects of such occlusions, the brain utilizes an auxiliary vascular network known as collateral circulation. These collateral pathways are broadly categorized into primary collaterals, such as the Circle of Willis, and secondary collaterals, including leptomeningeal anastomoses and ophthalmic arteries [3,4]. Their ability to reroute blood flow around the occluded regions can preserve the ischemic penumbra and significantly influence treatment outcomes [5]. More recently, the roles of venous and lymphatic pathways in maintaining intracranial homeostasis during ischemia have also been recognized [6].

Although reperfusion therapies like intravenous thrombolysis and mechanical thrombectomy have revolutionized acute stroke management, their effectiveness is time-sensitive. Patients with robust collateral circulation often experience slower infarct progression and may benefit from extended treatment timeframes [7–9]. As a result, the evaluation of collateral status has become a critical prognostic factor and a key determinant in clinical decision-making.

Traditionally, collateral assessment relies on imaging techniques such as Computed Tomography Angiography (CTA), magnetic resonance angiography (MRA), and, more recently, Cone beam computed tomography (CBCT). However, these assessments are often manual, subjective, and require considerable expertise, leading to inter-observer variability. To address these challenges, artificial intelligence (AI), particularly deep learning (DL), has gained momentum for automating collateral circulation classification. Deep learning models, especially convolutional neural networks (CNNs), have demonstrated outstanding performance in various diagnostic tasks, including pneumonia detection [10] and chronic kidney disease screening via retinal imaging [11], by automatically extracting high-level features from medical images.

In the context of ischemic stroke, deep learning holds the potential to transform collateral assessment by providing accurate, reproducible, and real-time evaluations. Recent studies have employed models such as ResNet and VGG to classify collateral quality from CTA, MRI, and CBCT data, achieving encouraging results. Moreover, the integration of multimodal fusion and hybrid CNN transformer architectures is further enhancing diagnostic accuracy, especially in complex clinical scenarios. Despite these promising advances, there remains a lack of a consolidated review that critically synthesizes both the physiological background of collateral circulation and the rapid progress of AI-driven classification methods. Previous reviews have largely focused on imaging modalities or stroke treatment outcomes in isolation, leaving a gap in integrating traditional and emerging AI approaches. By explicitly addressing this gap, this review provides timely insights into how collateral evaluation is evolving and why AI-based methods are gaining clinical importance.

This review is particularly relevant at the current stage, as recent studies have demonstrated the increasing feasibility of applying deep learning models in acute stroke workflows, yet challenges such as inter-observer variability, domain shift, limited external validation, and lack of standardized datasets persist. Highlighting these issues alongside technical advances not only clarifies the current state of the field but also sets directions for future clinical translation.

This review aims to synthesize recent advances in this evolving field and is structured around the following key areas:

- A comprehensive overview of the physiology and clinical importance of collateral circulation in ischemic stroke.
- Comparative analysis of imaging modalities, including CT, MRI, and CBCT, for evaluating collateral pathways.
- Review of existing collateral grading systems and scoring criteria used in clinical practice.
- Review of machine learning and deep learning techniques developed for collateral classification, including CNN, ResNet, VGG, and hybrid models.
- Performance metrics and benchmarking of DL models across recent studies.
- Clinical implications, challenges, and future directions for implementing AI-based collateral classification in stroke management.

Through this comprehensive review, we aim to highlight the potential of deep learning technologies to support and enhance the collateral assessment process, ultimately improving the prognosis and treatment outcomes for ischemic stroke patients.

2. Methods

The methodological approaches in this review aimed to ensure a transparent and structured synthesis of the literature on collateral circulation assessment and the use of artificial intelligence in ischemic stroke. This section details the search strategy, eligibility criteria, and the approach to data extraction and synthesis.

2.1. Search strategy and eligibility criteria

This review followed a structured approach to identify and synthesize evidence on collateral circulation assessment and the use of artificial intelligence for collateral circulation classification in ischemic stroke. The search was designed to capture the rapid growth of machine learning (ML) and deep learning (DL) applications in recent years, while also acknowledging earlier foundational contributions and guideline-based references. To ensure completeness, both peer-reviewed articles and key books were considered when they provided essential methodological insights or influential perspectives.

The literature search was conducted in PubMed, Scopus, Embase, and Web of Science, supplemented by manual screening of reference lists and relevant consensus statements. In total, 3,195 records were retrieved. Search terms combined concepts of ischemic stroke, collateral circulation, imaging modalities, and artificial intelligence, with a representative query formulated as: (Brain stroke OR ischemic stroke) AND (collateral OR collateral circulation) AND (CTA OR MRA OR CBCT) AND (deep learning OR machine learning OR CNN OR ResNet-50 OR VGG11). Syntax was adapted to meet the requirements of each database. Broader context was provided by international stroke guidelines and global burden reports [1,12,2,13,14].

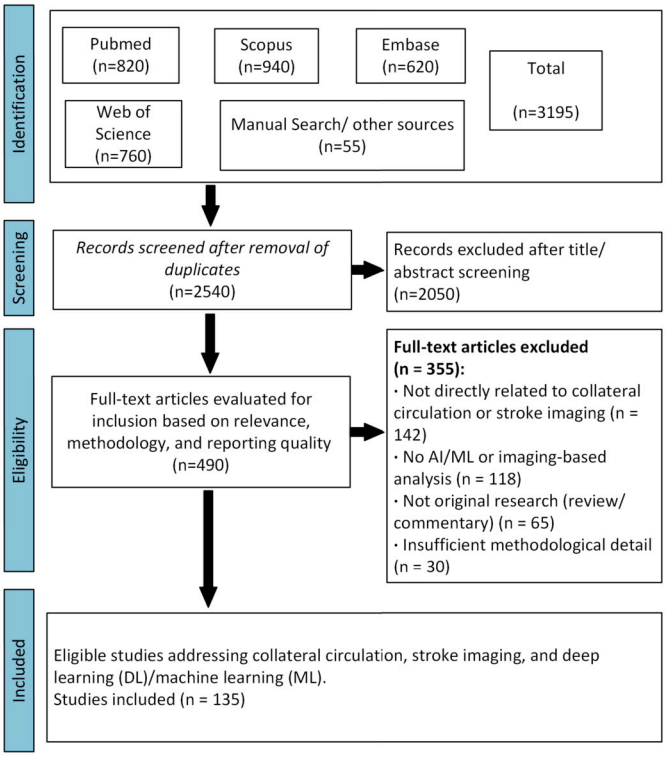

Fig. 1. PRISMA flow diagram summarizing identification, screening, eligibility assessment, and final inclusion of studies.

The selection process followed PRISMA recommendations. After removing 655 duplicates, 2,540 unique records remained for title and abstract screening. At this stage, 2,050 records were excluded because they did not meet the inclusion criteria. The full texts of 490 articles were then assessed for eligibility. Of these, 355 were excluded for the following reasons: not directly related to collateral circulation or stroke imaging (n = 142), absence of AI/ML or imaging-based analysis (n = 118), lack of original research such as reviews or commentaries (n = 65), or insufficient methodological detail (n = 30). Ultimately, 135 studies met all eligibility requirements and were included in the qualitative synthesis. These studies collectively addressed collateral circulation, stroke imaging, and the integration of AI/ML-based methods for collateral classification. The complete identification, screening, and inclusion process is presented in the PRISMA flow diagram (Fig. 1).

3. Brain stroke

Stroke occurs when the blood supply to a part of the brain is disrupted, leading to oxygen deprivation and rapid death of brain cells [15]. The brain is essential for coordinating movements, preserving memories, generating thoughts and emotions, and enabling speech and language functions [16]. It also regulates critical bodily processes such as breathing and digestion. To perform these functions effectively, the brain depends on a continuous flow of oxygen-rich blood delivered through its intricate arterial system. When this flow is blocked or reduced, brain tissue rapidly sustains damage [17]. Without timely restoration of blood supply, affected regions may suffer permanent injury or death, resulting in lasting disability or fatality. Strokes are broadly classified into two major types based on their underlying mechanisms: hemorrhagic stroke and ischemic stroke. Fig. 2 illustrates the fundamental differences between these two types.

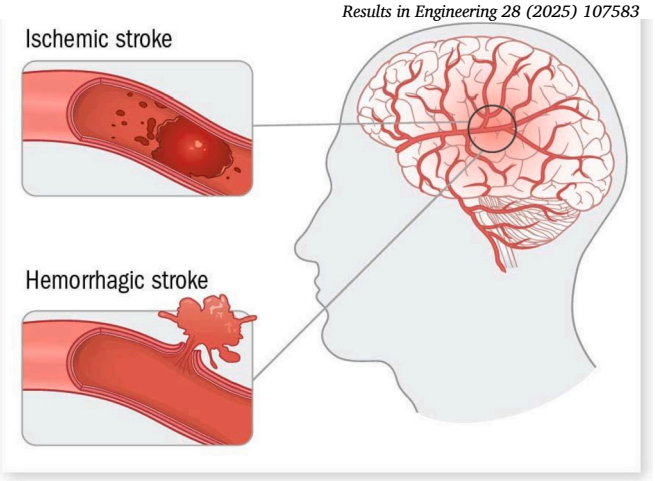

Fig. 2. Comparison between ischemic stroke (arterial blockage) and hemorrhagic stroke (vessel rupture) [18].

3.1. Hemorrhagic stroke

Hemorrhagic stroke occurs when a weakened blood vessel ruptures, causing bleeding into the brain tissue [19]. The accumulation of blood elevates intracranial pressure, compresses brain structures, and diminishes downstream blood flow. Although hemorrhagic strokes are less common than ischemic strokes, they are associated with higher early mortality rates. Management of hemorrhagic stroke focuses on controlling bleeding, alleviating intracranial pressure, and preventing complications such as rebleeding and hydrocephalus. Since hemorrhagic stroke arises from vessel rupture rather than occlusion, collateral circulation does not play a central role in its clinical management [20]. Accordingly, research into collateral blood flow restoration is less applicable to hemorrhagic stroke. Therefore, this review will primarily focus on ischemic stroke, where collateral circulation is critically important for tissue survival and recovery outcomes.

3.2. Ischemic stroke

Ischemic stroke, accounting for approximately 85% of all stroke cases, results from obstruction of a cerebral artery, most commonly due to thrombosis or embolism [21]. The sudden interruption of blood flow initiates a cascade of cellular injury and metabolic dysfunction, ultimately leading to infarction if untreated. Collateral circulation, the network of auxiliary vessels capable of supplying blood to ischemic brain regions, emerges as a crucial determinant of stroke severity and recovery potential [22]. Well-developed collateral networks can sustain perfusion to the ischemic penumbra, delay infarct progression, and extend the therapeutic window for interventions. Consequently, evaluation and optimization of collateral pathways have become major areas of clinical and research interest in ischemic stroke management.

3.3. Data extraction and analysis

Because of the wide variation in study designs, imaging modalities, collateral grading systems, and outcome reporting, a quantitative meta-analysis was not feasible. Instead, the data were synthesized narratively and thematically. Each study was charted according to its imaging modality (e.g., single- or multiphase CTA, MRA, CBCT), the collateral grading system employed ([23], [24], [25], [26]), the automation approach (radiomics, classical ML, or deep learning), and the model architecture implemented (e.g., CNN, ResNet, VGG, transformer, or hybrid). Reported outcomes, including accuracy, AUC, sensitivity, specificity, and F1-score, were systematically extracted.

Where available, additional methodological details such as dataset size, study setting (single- or multi-center), and the use of external

validation were also recorded, as these factors strongly influence the robustness and generalizability of AI models [27–30]. This thematic synthesis enabled the identification of patterns across imaging modalities and computational frameworks, while also highlighting areas of convergence and research gaps that warrant further investigation. Given these variations, the present work is reported as a narrative review rather than a systematic review or meta-analysis, and its aim is to synthesize current evidence while acknowledging the limitations in replicability and risk-of-bias assessment. Together, these steps provided the foundation for a structured narrative synthesis of the literature, which is presented in the following sections.

3.4. Gender-related stroke risk and outcomes

Gender significantly influences the incidence, presentation, and outcomes of stroke. Men tend to experience stroke at younger ages, whereas women often suffer strokes later in life, with higher rates of post-stroke disability and mortality [31,32]. Factors such as older age at onset and greater comorbidity burden contribute to poorer rehabilitation outcomes among women.

Moreover, unique risk factors, including pregnancy, preeclampsia, gestational hypertension, and hormone replacement therapy, further elevate stroke risk in women [33]. Women are also more likely to present with atypical symptoms, such as fatigue, confusion, or generalized weakness, potentially delaying diagnosis and treatment initiation [34]. Addressing these disparities through gender-sensitive prevention, diagnosis, and management strategies is essential for improving outcomes across all stroke patients. A comprehensive understanding of the types, progression, and risk factors associated with stroke, particularly ischemic stroke, provides a strong foundation for exploring the critical role of collateral circulation in influencing recovery outcomes. By emphasizing ischemic stroke and its dependence on collateral circulation, this review specifically advances beyond general stroke overviews by integrating the physiological basis of collaterals with recent AI-driven classification methods, highlighting both clinical potential and translational challenges.

While ischemic stroke dominates the global burden and outcomes vary by sex and risk profile, the single most modifiable imaging determinant of tissue fate is collateral blood flow. Because collateral adequacy governs infarct progression and influences IVT/EVT decision-making, the next section examines collateral circulation in detail its anatomy and physiology, how it is assessed on CTA/MRA/CBCT, and how these assessments underpin automated (AI) grading.

4. Collateral circulation in stroke

Collateral circulation refers to an auxiliary vascular network that compensates for impaired cerebral perfusion during arterial occlusion. These networks, primarily involving leptomeningeal anastomoses and pial arteries, redirect blood flow around the site of blockage, supplying oxygenated blood to the ischemic penumbra surrounding the infarct core [3]. This physiological response is critical for slowing infarct progression, limiting tissue damage, and extending the therapeutic optimal intervention period for interventions such as thrombolysis and thrombectomy [35,36].

Fig. 3 illustrates the anatomical principle of collateral circulation, showing how blood can reroute around a thrombus through smaller adjacent vessels. The efficiency of these collateral pathways varies considerably among individuals, influenced by factors such as vascular anatomy, age, comorbidities, and overall cerebrovascular health.

In clinical practice, collateral circulation is assessed using various angiographic techniques. While digital subtraction angiography (DSA) remains the gold standard due to its high spatial and temporal resolution, less invasive alternatives such as computed tomography angiography (CTA) and magnetic resonance angiography (MRA) are widely employed

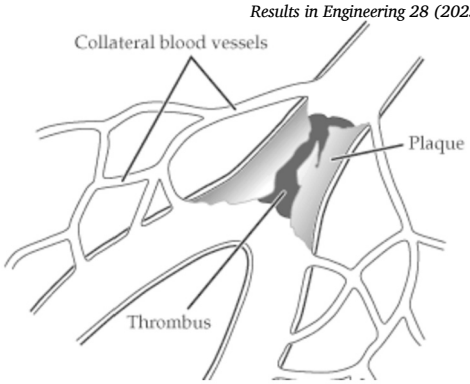

Fig. 3. Schematic showing collateral blood vessels bypassing a thrombus obstructing a primary cerebral artery [37].

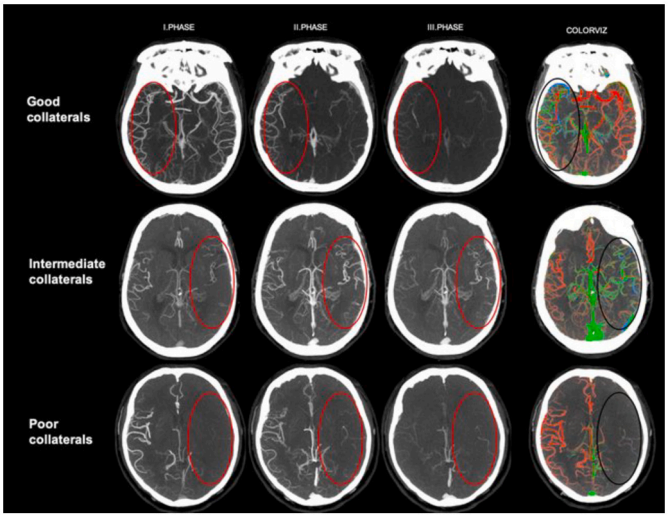

Fig. 4. Multiphase CTA based visual assessment of collateral circulation: good (top), intermediate (middle), and poor (bottom) collateral grades with corresponding color-coded visualization [40], (Image adapted under a CC BY 4.0 license.).

for rapid evaluation. Among these, multiphase CTA has gained particular importance, as it captures vascular filling over multiple time points, allowing visualization of delayed collateral recruitment [38]. Several collateral grading scales, such as those proposed by Seners and Gensicke have been developed to visually assess collateral status based on angiographic data [39,24]. These scales categorize collateral flow into classifications such as good, intermediate, or poor, providing valuable guidance for estimating infarct growth potential and informing acute treatment decisions. However, these methods remain largely qualitative, subject to inter-observer variability, and their reproducibility across centers is limited, which underscores the need for standardized and automated approaches.

Fig. 4 presents an example of multiphase CTA-based collateral scoring. The top row shows robust collateral filling across all three CTA phases, indicative of good collateral status. The middle row displays partial filling consistent with intermediate collaterals, while the bottom row demonstrates minimal collateral recruitment, classified as poor. The final column provides a color-based visualization for more intuitive grading.

Collateral circulation plays a significant role in determining clinical outcomes in ischemic stroke. Patients with well-developed collateral networks tend to have smaller infarct volumes, slower infarct expansion, and improved responses to reperfusion therapies [41]. Conversely, poor collateralization is associated with rapid infarct progression, an increased risk of hemorrhagic transformation, and worse functional out-

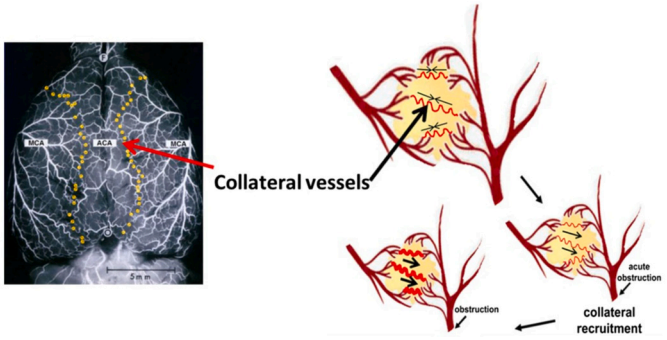

Fig. 5. Angiographic visualization of cerebral collateral vessels and flow enhancement strategies in acute ischemic stroke. Adapted from Biose et al. [45] (Translational Stroke Research, CC BY 4.0).

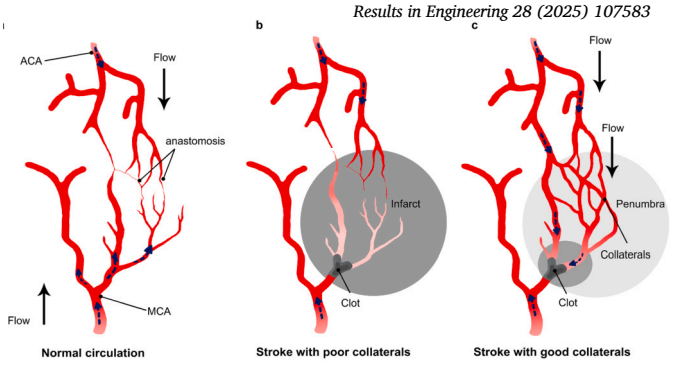

Fig. 6. Classification of collateral circulation: (a) Normal circulation, (b) Stroke with poor collaterals, (c) Stroke with good collaterals [47], International Journal of Molecular Sciences, CC BY 4.0 license.

comes [5]. Recent major clinical trials, such as ESCAPE and DEFUSE-3, have underscored the critical importance of collateral imaging. These studies demonstrated that patients with favorable collateral status could derive significant benefit from endovascular treatments even beyond the traditional 6-hour optimal intervention period [42,43]. Consequently, evaluation of collateral circulation has become an integral component of modern stroke triage protocols and personalized treatment strategies.

5. Physiological significance of collateral circulation in ischemic stroke

Collateral circulation plays a critical role in ischemic stroke by providing alternative pathways to sustain cerebral perfusion during arterial occlusion. These networks, consisting primarily of leptomeningeal anastomoses and pial arteries, dynamically compensate for compromised blood flow, directly influencing infarct progression, therapeutic time windows, and overall clinical outcomes. In addition to arterial collaterals, venous collateral pathways also contribute significantly to maintaining cerebral hemodynamics. While arterial networks help preserve perfusion pressure, venous collaterals facilitate drainage from congested brain regions, particularly under conditions of venous outflow obstruction [44]. Both systems are increasingly recognized as vital determinants of successful reperfusion therapy and favorable stroke recovery.

Fig. 5 provides an angiographic depiction illustrating the brain's adaptive collateral response during ischemia, highlighting the extensive vascular networks that become critical when primary arterial pathways are obstructed.

The clinical significance of collateral circulation extends beyond stroke to other vascular conditions, such as coronary and peripheral artery diseases, where collateral status informs revascularization strategies and prognosis. In the context of ischemic stroke, patients with well developed collateral networks consistently exhibit smaller infarct volumes, delayed infarct growth, and improved functional outcomes [46]. Furthermore, the preservation and enhancement of cerebral perfusion remain cornerstones of ischemic stroke therapy. Biose [45] emphasized that robust collateral circulation can effectively balance infarct expansion and tissue salvageability, thereby directly influencing recovery potential. In clinical workflows, the adequacy of collateral perfusion is increasingly recognized as the single most modifiable imaging determinant of tissue fate, influencing door-to-needle and door-to-groin decision timelines in acute stroke care. A practical classification of collateral status is illustrated in Fig. 6, comparing normal cerebral circulation with cases of stroke accompanied by poor or good collateralization. This visual framework supports clinicians in quickly evaluating the extent and effectiveness of collateral supply during acute stroke imaging. Understanding the physiological significance of collateral circulation provides a critical foundation for appreciating its role in acute stroke diagnosis, prognosis, and the development of targeted therapeutic strategies aimed at optimizing patient outcomes. The preceding section described where collaterals reside and how they are graded on CTA/MRA/CBCT. The next question is why they matter biologically: how collateral flow maintains perfusion, limits core expansion, and influences time-critical decisions in acute care.

6. Imaging modalities for collateral assessment

Accurate assessment of collateral circulation is essential for predicting stroke progression, guiding treatment strategies, and improving clinical outcomes. A variety of imaging modalities are employed for collateral evaluation, each offering distinct strengths and limitations depending on the clinical context. Computed tomography angiography (CTA) remains the most commonly utilized modality in emergency settings due to its widespread availability, rapid image acquisition, and high spatial resolution. Single-phase CTA provides an initial snapshot of vessel patency, while multiphase CTA captures dynamic blood flow across sever Across imaging modalities, practical performance is influenced by spatial and temporal resolution, protocol timing, contrast bolus administration, and scanner vendor settings, which together introduce variability affecting collateral conspicuity and reproducibility across centers.

CTA-based assessments have been incorporated into several visual collateral grading systems, such as those proposed by Tan and Maas. Complementing CTA, Magnetic resonance imaging (MRI), particularly magnetic resonance angiography (MRA) and perfusion weighted imaging (PWI), offers excellent soft tissue contrast without exposing patients to ionizing radiation. Although MRI is slower and less accessible in acute stroke settings compared to CT, it provides valuable information regarding both anatomical structures and cerebral hemodynamics. MRA is effective for non-invasive vessel visualization, while perfusion MRI aids in delineating the ischemic core and penumbra, indirectly reflecting collateral function [57].

CBCT has recently been introduced into neurointervention suites, building upon its extensive use in dental and interventional radiology contexts. CBCT provides high-resolution three-dimensional visualization of cerebral vasculature directly within the angiography suite, supporting intraoperative assessment (Fig. 7). Evidence from non-neuro domains suggests potential advantages in terms of spatial resolution, radiation exposure, and cost compared to conventional CT [58,59]. However, stroke-specific head-to-head comparisons between CBCT and multidetector CT remain limited. Accordingly, while CBCT shows promise for collateral evaluation during endovascular procedures, current claims regarding dose, cost, and workflow efficiency should be interpreted cautiously and viewed as preliminary until further neuro-focused studies are available. Accordingly, statements regarding radiation dose, scan time, and cost are restricted to the non-neuro CBCT literature cited here and are not asserted as established advantages in acute stroke pathways.

In the context of stroke imaging, CT remains the primary diagnostic tool, followed by MRI. Despite its utility, CT is associated with mod-

Table 1
General comparison of CBCT, CT, and MRI imaging characteristics. Reported values are mainly from dental/ENT and general radiology literature. Stroke- and neurointervention-specific, head-to-head evidence remains limited; therefore, these characteristics should be interpreted cautiously when extrapolated to acute cerebrovascular workflows.

Criteria	CBCT	CT	MRI
Working Principle	Uses X-ray computed tomography with divergent beam and 360° rotation [49]	Uses multiple X-rays from different angles [50]	Uses magnetic fields and RF pulses [51]
Resolution	High spatial resolution [49]	Better contrast resolution [49]	Good contrast resolution [51]
Scanning Time	Lower scanning time [52]	Moderate scanning time [52]	Longest scanning time [52]
Radiation Exposure	Lower radiation exposure [53]	Moderate radiation exposure [53]	No radiation exposure [53]
Image Accuracy	Provides isotropic voxels [54]	Anisotropic voxels [54]	Voxel size varies by protocol [55]
Imaging Artifact	Lower metal artifact levels [53]	Higher metal artifact levels [53]	High metal artifacts in certain cases [51]
Cost	Lower cost [56]	Moderate cost [56]	Highest cost [56]
X-ray Beam Coverage	Beam can be collimated to the area of interest [54]	Full area scan [54]	Full area scan [56]
Display Mode	High anatomical precision and diagnostic function [54]	Lower anatomical detail [54]	High-quality images for soft tissue and ligaments [51]

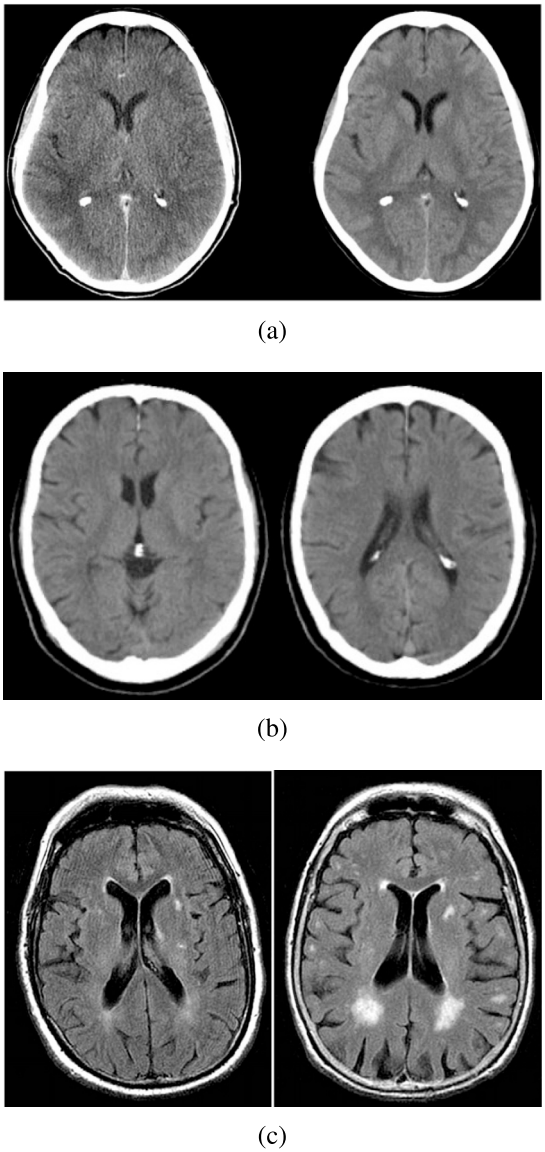

Fig. 7. Visual comparison of imaging modalities: (a) CBCT offers high spatial resolution and 3D visualization; (b) CT provides rapid, high-contrast views; (c) MRI delivers superior soft tissue contrast [48]. Illustrations are schematic and modality performance varies by protocol, scanner, and clinical workflow.

erate radiation exposure and notable cost considerations, while MRI although radiation-free and providing superior soft tissue contrast is slower and less practical for acute triage. CBCT may offer a complementary alternative within the angiography suite, providing real-time vessel visualization with high resolution. Nevertheless, most reported advantages of CBCT (e.g., lower radiation dose, shorter scan time, and reduced cost) are derived from non-neuro literature. A comparative overview of CBCT, CT, and MRI is provided in Table 1, which summarizes key imaging characteristics while noting that direct stroke-specific comparisons are still limited. Building on the modality overview, the next section reviews the visual collateral grading scales most used in practice (Tan, Maas, Miteff, ASITN/SIR), clarifies their definitions and ordinal structure, and outlines implications for dataset labeling, threshold selection, and validation of automated methods. Overall, CTA remains the first-line modality in the emergency setting, MRI provides complementary hemodynamic insights when feasible, and CBCT represents a promising intra-procedural tool; nonetheless, cross-center variability and the limited stroke-specific CBCT evidence highlight the need for standardized protocols and rigorous validation before widespread adoption.

7. Scoring systems for collateral circulation

Because these scales were developed on different cohorts and imaging phases, we present them in a harmonized, severity-oriented layout and explicitly note their ordinal structure and intended imaging context. A wide range of studies have introduced diverse scoring systems to evaluate collateral circulation in patients with acute ischemic stroke.

Despite extensive research, no universally accepted standard for collateral flow grading exists, leading to variability in assessment practices across clinical settings [67]. Each scoring system adopts its own set of criteria and classification thresholds, thereby influencing treatment decisions and prognostic interpretations. To provide a clearer understanding of how collateral quality is classified, Table 2 presents a comparative summary of the features distinguishing poor, moderate, and good collateral circulation. This comparison highlights key parameters across studies and underscores the ongoing lack of standardization in clinical evaluation. In practice, inter-observer variability persists even among experienced readers, particularly for intermediate grades, and multicenter reproducibility is sensitive to acquisition timing and windowing. For AI development and benchmarking, a pragmatic approach is to predefine mappings (e.g., 3-class poor/intermediate/good or 2-class poor vs. non-poor) with consensus labeling and adjudication, and to report per-class metrics alongside overall AUC/accuracy.

Several key studies have proposed different approaches for evaluating collateral circulation in ischemic stroke and related vascular conditions. Kunyi Li et al. [68] introduced a three-point grading scale based on the assessment of the middle cerebral artery (MCA) branches around the Sylvian fissure, offering a simple and rapid method for collateral evaluation in acute settings. Similarly, Chen et al. [60] explored collat-

Table 2
Collateral Circulation Classification by Severity Levels.

Miteff Collateral Assessment [25]
Poor: Only superficial MCA branches are reconstructed distal to the occlusion
Moderate: Some MCA branches are reconstructed
Good: Most MCA branches are reconstructed
Vertebral Venous Expansion [60]
Poor: External vertebral vein ≤ 25%
Moderate: ≥ 25%
Good: ≥ 50%
Vascular Reperfusion [61]
Poor: Minimal recanalization
Moderate: Partial recanalization
Good: Complete recanalization
Infarct Growth [36]
Poor: Extensive infarct growth despite pre-treatment
Moderate: Reduced infarct growth with pre-treatment
Good: No significant infarct growth with pre-treatment

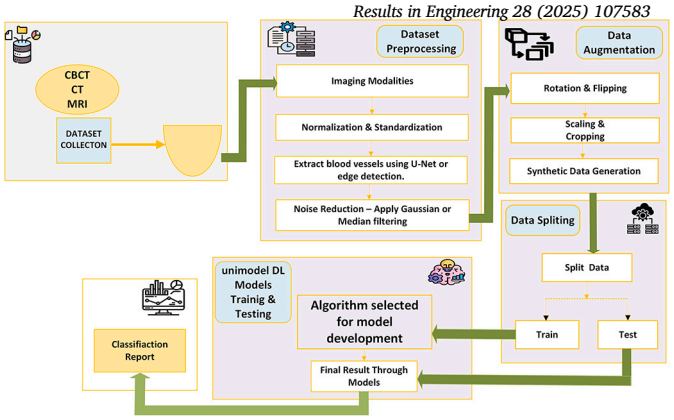

Fig. 8. Common approach for automatic collateral classification in ischemic stroke, including dataset collection, preprocessing, data augmentation, model development, and evaluation.

eral vessel classification in the context of chronic cerebrospinal venous insufficiency (CCSVI), using jugular ultrasound and contrast-enhanced magnetic resonance venography (CEMRV), thus extending collateral research beyond arterial systems. Uniken Venem et al. [36] demonstrated that pre-treatment collateral status significantly predicts revascularization outcomes following endovascular therapy. Patients with good or excellent collaterals achieved substantially higher rates of complete reperfusion. An earlier study by [61] also emphasized that poor collaterals independently predicted rapid infarct expansion based on MRI diffusion perfusion mismatch analysis. As shown in Table 2, robust collateral networks are associated with successful reperfusion and limited infarct expansion, reinforcing their critical prognostic role in acute stroke management.

Clinically, these scales stratify infarct growth risk and potential benefit from reperfusion, but their ordinal cutoffs should be interpreted in the context of phase timing and patient-specific factors (e.g., onset-to-scan time, vascular territory). Enhancing collateral circulation has therefore emerged as a key therapeutic strategy to improve outcomes in ischemic stroke. The integrity and adaptability of collateral vessels significantly influence infarct development and the success of reperfusion therapies. However, several physiological and external factors, such as antihypertensive medications, systemic vascular compromise, and pre-existing cerebrovascular dysfunction, may impair collateral function [69].

To address these limitations, various hemodynamic interventions have been explored to augment collateral perfusion. Strategies such as induced hypertension, volume expansion, head positioning in a flat posture, external counterpulsation, partial aortic occlusion, and sphenopalatine ganglion stimulation have been investigated to optimize ischemic penumbra perfusion and extend therapeutic windows [70]. Numerous collateral grading systems have been developed, particularly based on angiographic imaging. Table 3 Taken together, these frameworks are ordinal by design (e.g., absent → poor → intermediate → good) and differ in anatomical focus (e.g., MCA territory), phase timing (single vs. multiphase CTA), and visual thresholds. This heterogeneity complicates cross-study comparison and model training, and it partly explains the variability seen in downstream prognostic analyses. Summarizes the essential characteristics of commonly cited grading methods. While these frameworks provide valuable clinical insights, they largely rely on subjective visual interpretation. This introduces challenges such as inter-observer variability and the labor-intensive nature of manual grading. As Rava et al. [71] highlighted, such variability may compromise diagnostic consistency, particularly in time-sensitive clinical settings. Recent advancements advocate integrating neuroradiology expertise with artificial intelligence (AI) to automate collateral evaluation. Although promising developments are underway, significant human input is still required. Consequently, the proposal of simplified two-grade collateral frameworks aims to enhance reproducibility and streamline clinical application. In parallel, studies such as Su et al. [46] and Seners et al. [23] demonstrated that structured collateral grading systems can predict outcomes following endovascular thrombectomy (EVT), with higher collateral scores correlating to better functional recovery. Additionally, Markus et al. [64] highlighted the utility of early transcranial Doppler (TCD) evaluation within 24 hours, identifying patients with favorable collateral status. Gensicke et al. [24] and Rabinstein et al. [26] further reinforced the prognostic value of early collateral assessment via CT angiography in patients with MCA occlusion. Similarly, Seker et al. [25] and Kuang et al. [62] validated three-point grading scales that correlated strongly with clinical outcomes, although anatomical variability remains a challenge.

Collectively, these studies confirm that collateral circulation serves as a vital compensatory mechanism during arterial occlusion. Its accurate and timely assessment remains critical for optimizing treatment strategies and improving outcomes in acute ischemic stroke management. Because these visual scales are heterogeneous and ordinal, the next section details AI-based collateral classification pipelines and their evaluation. Because these visual scales are heterogeneous, qualitative, and time-sensitive, automated pipelines that respect the ordinal nature of grading and the spatiotemporal dynamics of multiphase imaging are a logical next step provided they are trained with consensus labels, externally validated, and calibrated for clinical decision support.

8. Collateral circulation classification techniques

This section outlines the standard workflow for automated collateral grading data acquisition, preprocessing, augmentation, model training, and evaluation, and compares common model families (CNN, ResNet18/50, VGG, transformers, and hybrids) in practical terms.

8.1. Model architectures for collateral classification

Most research studies on brain collateral circulation classification follow a standardized processing and modeling pipeline. As shown in Fig. 8, Schematic created by the authors. To support reproducibility, pipelines should predefine patient-level splits (to avoid leakage), stratify by class, and reserve a held-out external test set. We encourage bootstrapped 95% CIs for all metrics, reporting per-class sensitivity/specificity and macro-F1 in addition to AUROC. Domain shift should be anticipated (scanner vendor/protocol/phase timing); harmonization and external validation are therefore essential. The typical procedure begins with dataset collection from brain imaging modalities such as CBCT, CT, or MRI, classes.

The collected data undergoes a series of preprocessing steps, including normalization, standardization, vessel extraction (using methods

Table 3
Collateral Circulation Grading Systems by Other Researchers.

Author	Imaging Modality	Grading System Description
[46]	CT Angiography	0: Absent collaterals (0% filling); 1: Poor collaterals (>0% and ≤50% filling); 2: Moderate collaterals (>50% and <100% filling); 3: Good collaterals (100% filling).
[62]	CT Angiography	1: Good (100% collateral supply); 2: Intermediate (>50% and <100%); 3: Poor (≤50%).
[63]	CT Angiography	1: Poor; 2: Good.
[64]	Transcranial Doppler	Good: ≥2 vessels; Poor: ≤1 vessel.
[24]	CT Angiography	Five-point scale ranging from absent to exuberant collaterals.
[25]	CT Angiography	1 (Good): Full reconstitution; 2 (Moderate): Sylvian branches; 3 (Poor): Distal superficial branches.
[23]	CT Angiography	0: Absent; 1: <50%; 2: 51–99%; 3: 100% filling.
[65]	MRI	Grades include: Absent, Subtle, and Prominent collateral patterns.
[66]	Cerebral Angiography	Good: ≥3 MCA retrograde branches; Poor: <3 retrograde branches.
[26]	Cerebral Angiography	0–4 point collateral flow scale.

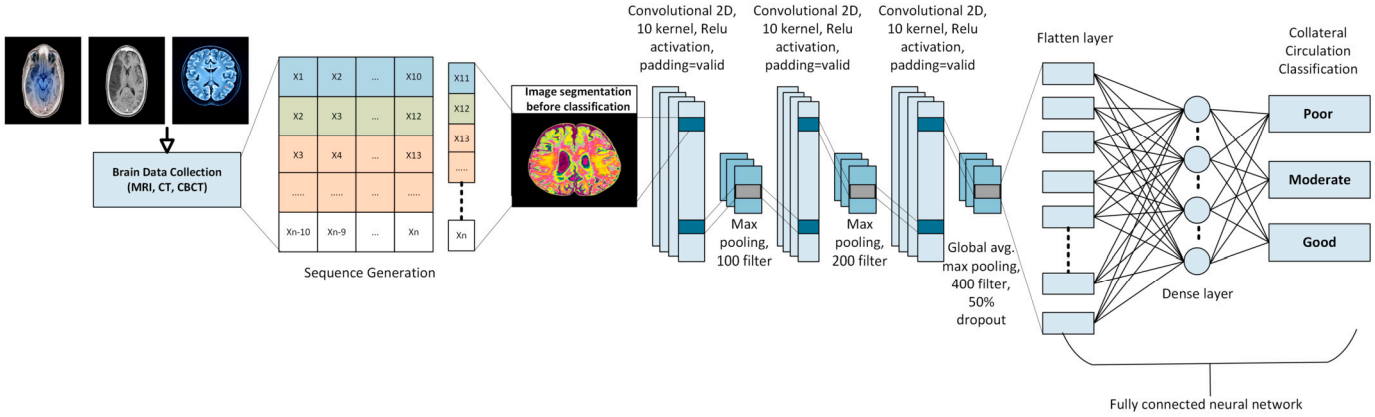

Fig. 9. Basic CNN architecture.

like U-Net or edge detection), and noise reduction through Gaussian or median filtering. To improve model robustness, data augmentation techniques such as rotation, flipping, scaling, cropping, and synthetic data generation are applied. The augmented dataset is then split into training and testing subsets, and selected unimodal deep learning models are trained and evaluated. Finally, the trained models produce classification reports, providing insight into the predicted collateral circulation, for ordinal targets (poor → intermediate → good), ordinal losses (e.g., CORN, cumulative link) or regression-to-grade with thresholding can reduce boundary errors versus flat softmax. Class imbalance can be addressed via focal loss, cost-sensitive weighting, or curriculum sampling, with thresholds selected by maximizing clinical utility rather than overall accuracy. Building upon this standardized pipeline, several deep learning model architectures have been employed for the classification task. Figs. 9 to 12 present representative models widely used in recent studies.

Fig. 9 presents the detailed structure of a typical Convolutional Neural Network (CNN) applied to collateral circulation classification. CNNs are a class of deep learning models designed specifically to process grid-like data, such as images, by automatically learning spatial hierarchies of features [72]. The architecture generally consists of an input layer receiving the raw imaging data (e.g., MRI, CT, CBCT), followed by a series of convolutional layers where filters slide across the input to capture local patterns. Each convolutional operation is typically followed by a non-linear activation function, such as ReLU (Rectified Linear Unit), which introduces non-linearity into the model and helps it learn complex representations [73].

Pooling layers (often max pooling) are interleaved between convolutional layers to progressively reduce the spatial resolution of feature maps, thus lowering computational cost and providing translational invariance [74]. As the data passes through successive convolutional and pooling layers, the model extracts increasingly abstract and high-level features from edges and textures in the early layers to complex anatomical structures in the deeper layers.

After feature extraction, the output is typically flattened and passed into one or more fully connected (dense) layers, which integrate the learned features across the entire input space. The final output layer employs a softmax activation function to assign probabilities across the predefined classes, such as 'poor,' 'moderate,' or 'good' collateral circulation categories.

One of the strengths of CNN architectures lies in their ability to perform end-to-end learning, eliminating the need for manual feature engineering [75]. Furthermore, by leveraging convolutional weight sharing and local receptive fields, CNNs maintain efficiency even when dealing with high-dimensional medical images. Studies such as Litjens et al. [76] and Shen et al. [77] have highlighted CNNs' effectiveness across a broad range of medical imaging tasks, including lesion detection, tissue segmentation, and disease classification. In collateral grading, CNNs benefit from vessel-centric priors (e.g., masks from U-Net or region proposals around MCA territory) and temporal stacking of multiphase CTA to capture delayed filling. Vessel-constrained saliency/Grad-CAM overlays should be provided to support clinician trust.

Fig. 10 illustrates the ResNet-50 architecture, a widely adopted deep convolutional neural network built on the principle of residual learning [78]. The core innovation in ResNet lies in the use of *identity shortcut connections*, which allow the input to skip one or more layers and be added directly to the output of stacked convolutional operations. This structure helps overcome the vanishing gradient problem that typically affects deeper networks, thereby enabling effective training of architectures with significantly increased depth.

The ResNet-50 model consists of 50 layers, organized into multiple convolutional stages. It begins with a 7×7 convolution with stride 2, followed by batch normalization and max pooling. The network then proceeds through four major stages comprising bottleneck blocks, where each block is made up of a sequence of 1×1, 3×3, and 1×1 convo-

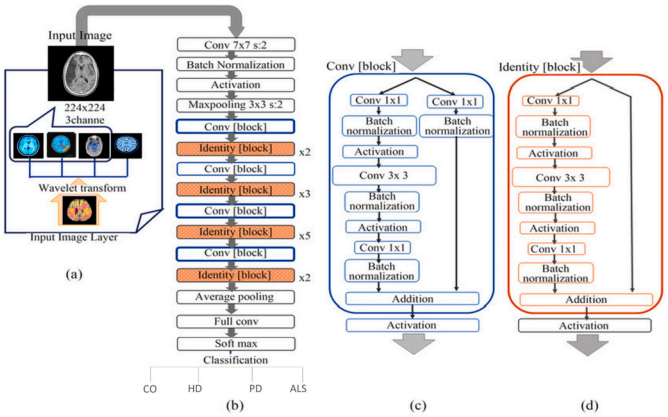

Fig. 10. ResNet-50 architecture.

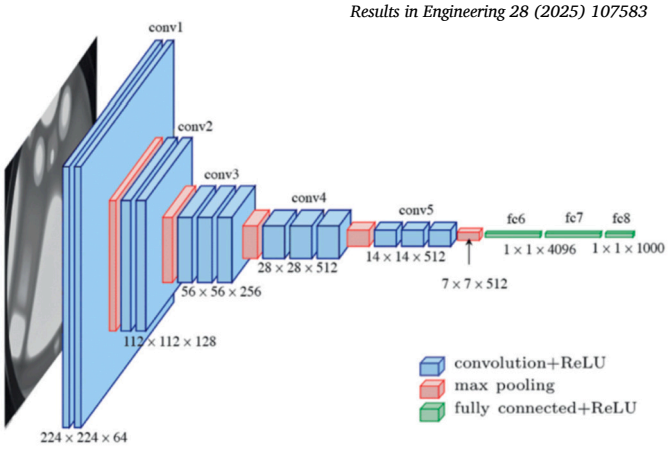

Fig. 11. VGG-11 architecture [83].

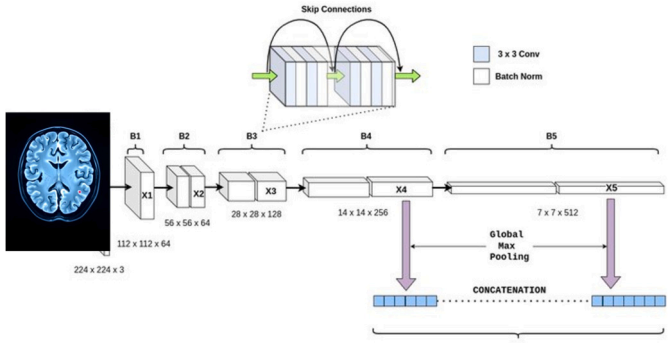

Fig. 12. ResNet-18 architecture.

lution layers. The initial 1×1 convolution reduces the dimensionality, the 3×3 layer performs spatial filtering, and the final 1×1 convolution restores dimensionality. This bottleneck design enhances computational efficiency while maintaining the model's ability to learn deep, rich feature representations.

As shown in the figure, residual connections are clearly indicated in the identity and convolutional blocks, allowing gradients to propagate more directly during backpropagation. The identity blocks (Fig. 10(d)) perform direct addition of inputs and outputs when the dimensions match, while the convolutional blocks (Fig. 10(c)) adjust dimensionality via learned transformations to enable valid addition.

The network concludes with an average pooling layer and fully connected layers, followed by a softmax classifier that outputs the probability distribution across the target classes, such as good, moderate, or poor collateral circulation in the case of ischemic stroke imaging.

ResNet-50 has demonstrated high accuracy and generalization across numerous medical imaging tasks, including lesion classification, stroke assessment, and vascular structure detection. Its residual design allows for deeper feature extraction without compromising training stability, which is particularly beneficial in biomedical contexts where subtle anatomical variations must be captured [79–81]. Trade-offs include higher compute and memory footprint; mixed-precision inference, model pruning, or knowledge distillation can reduce latency for real-time use. On limited datasets, transfer learning from medical imaging pretraining and strong regularization (stochastic depth, heavy augmentation) mitigate overfitting.

Fig. 11 highlights the VGG-11 architecture, a deep convolutional neural network proposed by Simonyan and Zisserman [82], known for its elegant and uniform design. Unlike residual networks such as ResNet, VGG-11 avoids shortcut connections and instead relies on a purely sequential stack of convolutional and pooling layers to progressively extract hierarchical features.

The architecture is built around repeated blocks of 3×3 convolutions with ReLU activations, each followed by max pooling operations. This uniform filter size allows the model to effectively capture fine spatial details while controlling the number of parameters. As shown in the figure, VGG-11 consists of five convolutional stages, each increasing in depth (number of feature maps) but reducing in spatial resolution, as the input progresses from $224 \times 224 \times 3$ to smaller dimensions through successive pooling layers.

After feature extraction, the output is flattened and passed through three fully connected layers (fc6, fc7, fc8), where the final fc8 layer produces class scores, often using a softmax activation to generate probabilities across the target categories. This structure makes VGG-11 particularly well-suited for classification tasks on structured and moderately sized datasets.

Despite its simplicity, VGG-11 has shown strong generalization capabilities in medical image analysis, including applications in brain imaging, lesion classification, and diagnostic assessment [84,85]. The model's sequential nature, combined with its depth, enables it to learn complex visual patterns while maintaining interpretability, though it typically requires more computational resources and training time compared to architectures with residual connections.

Fig. 12 presents the ResNet-18 architecture, a compact residual network designed to balance computational efficiency with strong feature learning capabilities [78]. Like its deeper counterparts, ResNet-18 incorporates identity shortcut (skip) connections, which allow the network to bypass certain layers during forward and backward propagation, effectively mitigating the vanishing gradient problem and facilitating smoother optimization in deeper models.

ResNet-18 consists of an initial 7×7 convolution followed by max pooling, then a series of four residual blocks, each containing two 3×3 convolutional layers. As shown in the figure, the feature map resolution progressively decreases while the number of filters increases, transitioning from $112 \times 112 \times 64$ to $7 \times 7 \times 512$. After feature extraction, global max pooling is applied, reducing the spatial dimensions and producing a compact feature vector, which is concatenated and passed to the fully connected layer for final classification.

Despite having fewer layers compared to ResNet-50, ResNet-18 has been widely adopted in medical imaging tasks, including stroke classification and brain lesion detection, due to its lower computational demands and faster inference times [86,87]. This makes it particularly suitable for real-time clinical applications or deployment on devices with limited hardware resources, without significantly compromising accuracy.

Fig. 13 depicts the machine learning (ML) pipeline used for classifying collateral circulation status into poor, moderate, or good categories based on structured features ($X1$, $X2$, $X3$, $X4$) derived from imaging or clinical data. The output variable (Y) represents the ground truth labels obtained from expert assessment or reference standards.

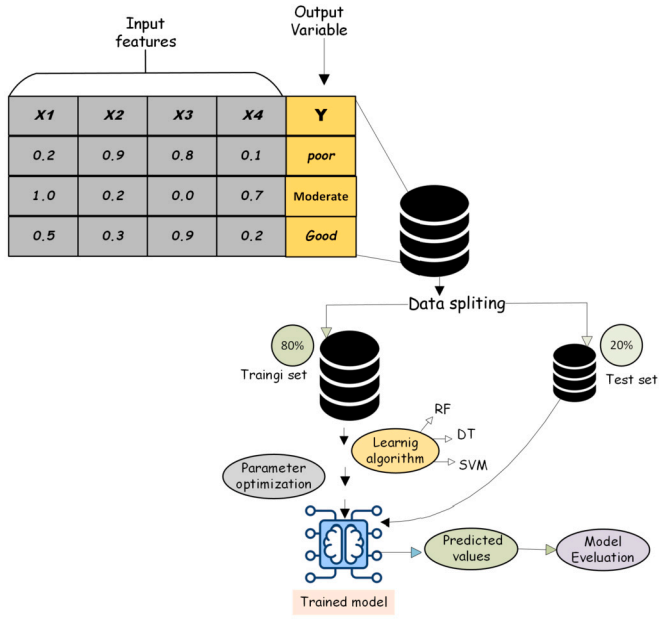

Fig. 13. Machine learning workflow for collateral classification using structured clinical and imaging features.

The dataset undergoes a standard data-splitting process, with typically 80% allocated for training and 20% for testing. During the training phase, supervised learning algorithms such as Random Forest (RF), Decision Tree (DT), and Support Vector Machine (SVM) are employed. These algorithms are optimized through parameter tuning to maximize predictive performance. Once trained, the model generates predicted values on the test set, which are subsequently evaluated using performance metrics such as accuracy, sensitivity, specificity, and F1-score [88,89].

Unlike deep learning models that require large datasets and raw image inputs, ML approaches rely on predefined features, offering faster training times, lower computational demands, and better interpretability. This makes them particularly appealing in clinical research settings where feature sets are carefully curated and dataset sizes are often limited.

Overall, to enable fair comparison across architectures, we recommend (i) reporting per-class sensitivity/specificity, macro-F1, AUROC with 95% CIs; (ii) ordinal agreement metrics (weighted Cohen's kappa, Spearman's ρ); (iii) calibration error (ECE) and Brier score; and (iv) external validation across distinct institutions/scanners. The summarized architectures in Table 4 reflect the prevailing trends in collateral circulation classification research. Among deep learning approaches, Convolutional Neural Networks (CNNs), ResNet-50, ResNet-18, and VGG-11 are the most commonly employed due to their strong ability to extract hierarchical and complex features directly from imaging data. These models have repeatedly demonstrated high classification accuracy, particularly in tasks involving stroke assessment and vascular characterization, thanks to their capacity for end-to-end learning and robust feature representation.

On the other hand, machine learning models such as Support Vector Machine (SVM), Random Forest (RF), Decision Trees (DT), and k-Nearest Neighbor (k-NN) continue to play an essential role, especially when working with structured clinical and handcrafted imaging features. These models are favored in studies with smaller datasets or where computational efficiency and interpretability are prioritized.

Together, these architectures provide a comprehensive toolkit for advancing the automated classification of brain collateral circulation, supporting improved clinical decision-making in ischemic stroke management. The integration of both deep learning and machine learning models underscores the importance of balancing data-driven feature learning with classic algorithmic strategies, depending on the nature of the available data and the specific clinical objectives. Building on the pipeline and architectures above, the next subsection surveys recent studies covering datasets, modalities, labeling strategies, validation scope, and reported performance and highlights persistent gaps

8.2. Recent studies in collateral circulation classification

Despite its significant potential, the application of deep learning in collateral circulation classification remains relatively limited, with only a handful of studies specifically targeting this domain using medical imaging modalities such as CT angiography and MRI. Table 5 summarizes key studies that have implemented deep learning approaches for collateral detection and classification in ischemic stroke patients. These automated methods assist radiologists in decision-making and pave the way toward real-time, AI-augmented clinical workflows. Tetteh et al. [103] comprehensively investigated the use of deep reinforcement learning for region of interest (ROI) identification from MR perfusion imaging parametric maps to improve the precision and interpretability of collateral assessment. Their study incorporated advanced feature extraction techniques, including three-dimensional Histogram of Oriented Gradients (3D HOG), Local Binary Patterns (LBP), and denoising autoencoders, which were subsequently fed into classifiers such as CNNs, Random Forests, and k-Nearest Neighbors (k-NN), demonstrating the effectiveness of combining deep and traditional machine learning methods.

Further advancements were introduced by Bağcılar et al. [105], who developed a hybrid CNN-Transformer framework to capture both local spatial features and long-range dependencies from CTA images, achieving robust performance across multiple evaluation metrics. Their study also revealed that clinical variables such as onset to CT time, NIHSS scores, gender, and age significantly influenced collateral status, supporting the clinical relevance of multimodal integration. Rava et al. [71] proposed a deep learning model using Keras and TensorFlow to predict collateral scores from arterial volume measurements extracted from CT perfusion imaging, demonstrating improved reproducibility over manual methods. Similarly, Hokkinen et al. [59] designed a 3D CNN to predict infarct core volume from CTA data, offering a strong correlation with final infarct volumes in late-window patients, thus highlighting the potential utility of non-contrast imaging in collateral evaluation. In parallel, Aziz et al. [106] evaluated conventional machine learning classifiers (Decision Tree, SVM, Random Forest, k-NN) on CBCT images, showing that SVM combined with Gray-Level Co-occurrence Matrix (GLCM) features yielded the best performance. Su et al. [46] combined CNN-based vessel segmentation and morphological feature extraction to classify collaterals in CTA images, demonstrating the advantages of hybrid pipelines combining deep learning and traditional feature-based methods. Clinically, multimodal fusion is most compelling when it reduces time-to-decision (door-to-needle/groin) and supports EVT selection; reporting should therefore include workflow timings and decision-impact, not only accuracy/AUC.

Meanwhile, Aktar et al. [107] proposed the ACCESS framework to assess collaterals based on the proportion of unenhanced vessels, offering a practical solution to minimize inter-observer variability in visual scoring. Oman et al. [108] utilized a 3D CNN architecture that integrated information from both non-contrast CT and contralateral hemispheres, improving lesion detection accuracy in early stroke assessment. Ali et al. [111] explored CBCT-based collateral classification using a VGG11 CNN model. Although the model achieved moderate accuracy (58.32%) with higher sensitivity (75.50%), it faced challenges related to data heterogeneity and moderate overfitting. Future improvements were suggested through the adoption of larger, multi-center datasets and deeper architectures like VGG16 or ResNet variants. Grunwald et al. [109] validated an automated collateral scoring system based on conventional machine learning, achieving high agreement with expert radiologists. Tangwiriyasakul et al. [104] developed a deep generative inference model using variational autoencoders to map NIHSS subscores

Table 4
Summary of Machine Learning and Deep Learning Model Architectures Used for Collateral Classification.

Model	Key Architecture/Working Principle	Notable Features	Reference
CNN (Basic)	Convolution → ReLU → Pooling → Fully Connected layers	Effective deep feature extraction; spatial pattern recognition for medical images	[90–92]
ResNet18	Conv1 layer followed by BasicBlock ×2 at four stages, then Fully Connected layer	Lightweight residual network; suitable for real-time applications; identity shortcuts for gradient stability	[78,93]
ResNet50	Conv1 layer followed by Bottleneck ×3, Bottleneck ×4, Bottleneck ×6, and Bottleneck ×3, then Fully Connected layer	Deeper architecture with bottleneck design; optimized for high-complexity image tasks	[78,81]
VGG11	Sequential Conv3×3 layers with MaxPooling at intervals, ending with Fully Connected layers	Simple and deep architecture; uniform convolution kernels; effective for smaller datasets	[82,94,95]
SVM	Finding the optimal hyperplane for separating classes in high-dimensional space	Robust for smaller datasets; highly effective with engineered features	[96,97]
Random Forest	Ensemble learning combining multiple decision trees using majority voting	Reduces overfitting; highly robust to noise and outliers	[98,99]
K-NN	Classifies samples based on the majority label among the k nearest neighbors in feature space	Simple, intuitive algorithm; sensitive to feature scaling and outliers	[100]
Decision Tree	Hierarchical recursive partitioning of data using learned decision rules	Easy to interpret; fast but prone to overfitting if not pruned appropriately	[101,102]

Table 5
Collateral Analysis Techniques by Other Researchers.

Study	Purpose	Imaging Modality	Technique	Result
[28]	Classification	4D-CTA	ResNet34 (Single-image and Multi-image Input)	Single-image model = 0.85, Multi-image model = 0.89
[27]	Classification	CTA	Multilevel Multimodal Deep Learning (CNN, Multimodal Fusion, AutoML)	Multilevel-Multimodal = 91.17%, CNN-Multimodal Fusion = 94.11%
[29]	Classification	Multi-phase CTA	Feature Fusion Attention Network (CCA4CTA) with Local and Global Attention	Accuracy = 90.43%
[104]	Collateral Mapping	CTA	Deep Generative Inference	Accurate localization of perfusion deficits
[103]	Classification	MRI	CNN, Random Forest, k-NN, SVM	CNN+MLP = 0.72, RF = 0.67, KNN = 0.44, SVM = 0.51
[105]	Classification	CTA	Hybrid CNN-SVM, ResNet, MViTv2, MPViT	SVM = 0.6774, ResNet = 0.7358, MViTv2 = 0.6246, MPViT = 0.767
[71]	Classification	CTA	CNN (Keras)	Accuracy = 0.76
[59]	Classification	CTA	3D CNN	Sensitivity = 0.38, Specificity = 0.89
[106]	Detection	CBCT	Decision Tree, SVM, Random Forest, KNN	DT = 0.77, SVM = 0.77, RF = 0.78, KNN = 0.68
[46]	Classification	CTA	CNN	Accuracy = 0.80
[107]	Detection	CTA	Conventional Machine Learning	Accuracy = 0.84
[108]	Detection	CTA	3D CNN	Sensitivity = 0.93, Specificity = 0.82
[109]	Detection	CTA	Conventional Machine Learning	Accuracy = 0.90
[110]	Core Volume Classification	CT Perfusion (CTP)	End-to-End CNN using VGG19 + 1D convolutions for spatial-temporal features	ROC-AUC = 0.72 (CV), 0.61 (external test)
[111]	Classification	CBCT	VGG11-based CNN	Accuracy = 58.32%, Sensitivity = 75.50%, Specificity = 44.10%, Precision = 52.70%, F1 = 62.10%
[30]	Classification	CTA	Radiomics + Ridge feature selection + XGBoost	AUC = 0.77 and 0.78 for binary classifications
[112]	Classification	CBCT	ResNet18	Accuracy = 65.9%, Sensitivity = 77.6%, Specificity = 52.6%, Precision = 65.0%, F1-score = 69.8%

from perfusion maps, introducing a novel non-invasive method for functional outcome prediction. Wang et al. [28] utilized stitched multi-phase CTA images combined with ResNet34, demonstrating that single-image models achieved a superior AUC of 0.89 for collateral classification. Raj et al. [27] advanced the field by integrating CNN features, vessel area metrics, and structural similarity measures (SSIM) through an AutoML ensemble, achieving 94.11% accuracy, thus showcasing the power of multimodal learning in stroke imaging. Avery et al. [30] applied radiomics feature extraction and machine learning classifiers (XGBoost) on CTA images, achieving AUCs of 0.77–0.78, and highlighted the independent prognostic value of radiomics-based collateral scores. [110] proposed an end-to-end deep learning model using VGG19 and temporal 1D convolutions for infarct core volume classification directly from CTP data, reaching a mean ROC-AUC of 0.72 across cross-validation cohorts. Finally, Ali et al. [112] introduced a ResNet18 model for CBCT-based collateral classification, achieving 65.9% accuracy and emphasizing the benefits of residual learning in limited data scenarios. Across these studies, the adoption of deep learning, hybrid architectures, and multimodal strategies has shown substantial promise in automating collateral circulation assessment, ultimately supporting timely stroke diagnosis and intervention. Having reviewed recent methods and performance, the next section turns to clinical application, how pre-treatment collateral status informs triage and therapy selection (intravenous thrombolysis (IVT) and endovascular thrombectomy (EVT), predicts infarct growth and complications, and where AI-derived grades can influence workflow and outcomes.

9. Clinical applications: insights from collateral status

The assessment of collateral status offers crucial insights into the underlying mechanisms of large vessel occlusions (LVOs) in ischemic stroke. A particularly important contributor, often observed in specific ethnic groups, is intracranial atherosclerotic disease (ICAD), which can lead to stroke through mechanisms such as hypoperfusion caused by progressive arterial narrowing. Unlike acute embolic occlusions that develop abruptly, ICAD frequently results in chronic ischemia, which promotes the gradual formation or recruitment of collateral networks. This distinction aligns with previous pathophysiological findings, where both structural and functional imaging evaluations of collateral pathways have been explored as tools for distinguishing stroke etiologies

[113–115]. Operationally, collateral patterns can support early etiologic triage (ICAD versus embolic) and guide periprocedural planning (e.g., need for angioplasty/stenting, antiplatelet strategy), reinforcing the value of standardized collateral reads in real-time decision pathways.

Additionally, a recent meta-analysis focusing on patients undergoing reperfusion therapy revealed that strokes due to large artery atherosclerosis were significantly more likely to exhibit good pre-treatment collateral status compared to those of cardioembolic origin (risk ratio 1.24; 95% CI 1.04–1.50; P = 0.020), although notable heterogeneity across studies was observed [116]. Given the between-study heterogeneity, these effect estimates should be interpreted as hypothesis-generating; future analyses should stratify by occlusion site, treatment window, and grading scale, and adjust for baseline core, ASPECTS, NIHSS, and onset-to-imaging time.

10. Collateral circulation as a prognostic factor in ischemic stroke

Collateral circulation serves as a pivotal prognostic factor influencing both imaging findings and clinical outcomes in ischemic stroke patients. Data show that individuals presenting with poor collateral status upon admission often have larger ischemic core volumes and experience less favorable clinical progressions [129]. In contrast, within the initial 48-hour period following stroke onset, robust collateral flow has been associated with early neurological improvements and reduced rates of hemorrhagic transformation, whether symptomatic or asymptomatic [36].

In large prospective cohorts of LVO patients, the presence of strong collateral networks has emerged as an independent predictor of long-term favorable outcomes, particularly in those who do not receive reperfusion therapy. Interestingly, while collateral status has not been consistently linked to penumbra size, it has shown a strong association with ischemic core volume and the rate at which the core expands, as demonstrated by multimodal CT imaging analyses [130,131].

However, it is important to note that the prognostic value of collateral quality may not apply in the same way to ICAD cases, where stroke events often represent the collapse or exhaustion of the collateral reserve. While current data supporting this notion are limited, retrospective analyses, including those from the Warfarin-Aspirin Symptomatic Intracranial Disease (WASID) trial, suggest that collateral status independently predicts the risk of subsequent strokes in the affected vascular territory [132].

10.1. Prognostic role in intravenous thrombolysis

A comprehensive systematic review and meta-analysis, encompassing 25 retrospective cohorts and three post-hoc randomized controlled trial analyses with a combined total of 3,057 patients, reported that individuals with good pre-treatment collaterals were significantly less likely to experience symptomatic hemorrhagic transformation (risk ratio 0.38; 95% CI 0.16–0.90; P = 0.03). Furthermore, these patients exhibited higher rates of early neurological improvement (risk ratio 4.21; 95% CI 1.57–11.28; P = 0.004) and better functional outcomes, defined as mRS 0–2 at 3–6 months (risk ratio 2.45; 95% CI 1.94–3.09; $P < 0.001$). Other notable findings included lower median NIHSS scores at admission and smaller infarct volumes on baseline imaging. Interestingly, the analysis did not find statistically significant associations between collateral status and successful recanalization, reperfusion, overall hemorrhagic transformation risk, final infarct size, or three-month mortality [133].

11. Prognosis in endovascular thrombectomy

A substantial body of research has demonstrated the prognostic importance of collateral circulation in patients undergoing endovascular thrombectomy (EVT) for ischemic stroke. Two influential systematic reviews and meta-analyses, encompassing studies published through March 2015, showed that patients with good collateral status prior to EVT were significantly more likely to achieve successful reperfusion (as assessed by the modified Thrombolysis in Cerebral Infarction, mTICI, score; risk ratio 1.28, 95% CI 1.17–1.40, $P < 0.001$) and successful recanalization (measured by the Arterial Occlusive Lesion, AOL, score; risk ratio 1.23, 95% CI 1.06–1.42, P = 0.006) [133]. Additionally, good collateral status was associated with higher rates of favorable 90-day functional outcomes (mRS ≤ 2; risk ratio 1.98, 95% CI 1.64–2.38, $P < 0.001$), lower risk of symptomatic intracranial hemorrhage (risk ratio 0.59, 95% CI 0.43–0.81, P = 0.001), and reduced 90-day mortality (risk ratio 0.49, 95% CI 0.38–0.63, $P < 0.001$).

To improve comparability, we summarize studies with attention to scale used, window, and outcome definitions, and—where reported—include effect sizes with confidence intervals. Table 6 compiles landmark studies published after March 2015 [117,23,118,134,120–122,5,123,38,124,125,25,24,126–128,119], which consistently report a positive association between collateral status and outcomes in anterior circulation LVO. However, outcomes for vertebrobasilar LVO remain more variable, as highlighted by recent reviews [135].

Specifically, among patients treated in the late time window (6–24 hours after symptom onset), stronger collateral circulation has been associated with smaller computed tomography perfusion (CTP) core volumes, smaller penumbra, larger mismatch ratios, lower hypoperfusion intensity, and overall superior functional outcomes [119,112].

Pre-treatment collateral status consistently guides triage and therapy selection (intravenous thrombolysis and endovascular thrombectomy), predicts infarct growth and hemorrhagic risk, and correlates with functional outcomes. However, routine practice still depends on manual CTA/MRA/DSA grading with heterogeneous scales (Tan, Maas, Miteff, ASITN/SIR), variable phase timing, and only moderate inter-observer agreement; evidence for CBCT in the acute setting remains sparse. Most AI studies are retrospective, single-centre, and small, with limited external validation, scant calibration/uncertainty reporting, and minimal inclusion of clinical covariates or posterior-circulation/ICAD subgroups. This gap links the clinical need to the automated pipelines reviewed earlier: robust, ordinal, spatiotemporal AI that renders vessel-centred overlays with calibrated poor/intermediate/good outputs, abstains on low-confidence cases, and integrates into PACS/angiography workflows. Bridging this gap will require harmonised labeling across scales, multicentre datasets (including CBCT), and prospective evaluations that track workflow KPIs and patient outcomes. The Discussion synthesizes these issues, pinpoints remaining barriers (data, labeling, domain shift, workflow engineering), and outlines pragmatic routes to clinically deployable, real-time collateral classification.

12. Discussion

This review highlights the growing utilization of artificial intelligence, particularly deep learning (DL) methodologies, for classifying collateral circulation in ischemic stroke. Across recent studies, several significant trends and methodological innovations have emerged, underscoring the transformative potential of intelligent approaches in clinical diagnostics and therapeutic decision-making. As demonstrated in recent literature, CNN-based architectures have become the primary choice for collateral circulation classification, leveraging their exceptional ability to extract complex spatial and structural features from medical images. Notably, CNN variants such as ResNet34, ResNet18, ResNet50, and VGG11 have been widely employed due to their proven effectiveness in medical imaging tasks. For instance, Wang et al. [28] utilized a ResNet34 model on multi-phase CTA data, significantly improving classification performance by incorporating multiple temporal phases to capture dynamic collateral flow characteristics. Beyond architectural choice, multiphase inputs consistently improve discrimination by capturing delayed filling; however, across studies this gain is sensitive to protocol (single vs. multiphase CTA) and label granularity, underscoring the need for standardized acquisition and grading.

Table 6
Selected studies reporting the association between pre-treatment collateral status and outcomes after EVT of anterior circulation large vessel occlusion stroke.

Study	Patients (n)	Collateral scale (method)	Main findings
[117]	1,764 (871 EVT, 893 control)	Tan et al. [23] (sCTA, mCTA, CE-MRA)	Benefit seen across all strata; poor collaterals benefited less from EVT (not statistically significant).
[118]	130 (65 EVT, 65 control)	Tan et al. [23]	Good collaterals linked to smaller ischemic core volume and less growth; no significant link with outcome, sICH, or death.
[119]	161 (91 EVT, 70 control)	Tan et al. [23] (CTA), ASITN/SIR [5] (DSA)	Collateral status linked to infarct core at 24h, ASPECTS, successful revascularization, functional outcome, and death.
[120]	93	Tan et al. [23]	Good collaterals significantly linked to good clinical outcome (OR 9.69; P = 0.001).
[121]	104	Tan et al. [23]	Good collaterals linked to smaller final infarct, better NIHSS at 24h, lower in-house mortality; no link to 3-month mortality or outcome.
[122]	135	Tan et al. [23] (CTA), Christoforidis et al. [5] (DSA)	Good collaterals linked to better outcome (OR 2.13; $P < 0.001$), lower mortality, lower sICH, higher ASPECTS, better NIHSS.
[123]	119	Regional collateral scoring [38]	Good collaterals predicted good functional outcome (OR 5.14; P = 0.005).
[124]	339 (257 EVT, 82 no EVT)	Tan et al. [23]	EVT benefit (infarct growth, outcome, mortality) higher in poor collaterals.
[125]	84	Tan et al. [23] (CTA), Maas et al. [24] (CTA)	Good collaterals in Miteff/Maas scores linked to good outcome.
[126]	283	Miteff et al. [25] (sCTA)	Collateral grade linked to final infarct volume, but not to the functional outcome.
[127]	361 (285 EVT, 76 medical)	CTA [38]	Collateral status linked to early infarct growth, which links to functional outcome.
[128]	2,020	ASITN/SIR (DSA)	Good collaterals linked to successful reperfusion (OR 1.77), excellent reperfusion, good outcome; not linked to sICH or 3-month mortality.

Similarly, Ali et al. [112], [111] employed ResNet18 and VGG11 architectures, respectively, demonstrating competitive results despite challenges posed by limited and heterogeneous CBCT datasets, Generalization remains the key barrier: most results are single-center without external validation, and domain shift (scanner vendor/protocol, case-mix) can degrade performance. Future datasets should be multi-center with predefined external test sets. Thus underscoring the robustness and adaptability of these CNN models in diverse imaging scenarios. Expanding further, hybrid models combining CNNs with Transformers or multimodal feature fusion have been increasingly favored by researchers. These models integrate the superior local feature extraction capabilities of CNNs with the global contextual understanding of Transformer-based architectures, significantly enhancing overall performance. Bağcılar et al. [105], for instance, successfully combined CNNs with the MPViT transformer architecture, achieving superior accuracy compared to conventional ResNet and SVM classifiers by effectively capturing both local and global contextual features from CTA images. Raj et al. [27] further illustrated the advantage of employing multimodal fusion strategies, integrating CNN-extracted structural features with AutoML-based texture metrics. This multilevel fusion strategy significantly enhanced classification accuracy, reflecting the benefits of simultaneously leveraging diverse data streams to improve diagnostic precision.

To aid reproducibility and comparison, we harmonize reporting around accuracy, AUC, sensitivity, specificity, and F1, and note where thresholds or class balance differ across studies. As shown in Table 7, a range of intelligent assistant frameworks has been employed to automate collateral classification. CNN-based architectures are the most dominant, owing to their capacity for high-dimensional feature extraction from imaging data such as CTA, CBCT, and MRI. In addition, hybrid methods incorporating Transformer-based architectures (e.g., Multi-Path Vision Transformer (MPViT)) and AutoML pipelines have shown improved accuracy and robustness. Traditional machine learning techniques, such as SVM, k-NN, and Random Forest, remain relevant when applied to structured features, particularly when datasets are limited or when interpretability is required. These strategies collectively demonstrate that deep learning is at the forefront of innovation in this domain, while hybrid and conventional methods still serve as valuable complementary tools.

Table 7
Most Common and Effective Models for Collateral Circulation Classification.

Model Type	Purpose
CNN models (ResNet34, VGG11, ResNet18)	Automated classification from CTA, CBCT, MRI [28,112,111]
Hybrid CNN-Transformer (MPViT, MViTv2)	Spatial and long-range feature fusion [105]
CNN + AutoML Fusion	Structural + texture-based evaluation [27]
Deep Generative Inference Model	Mapping NIHSS from perfusion maps [104]
Traditional ML models (SVM, RF, k-NN)	Morphology-based classification [106,103]

The evaluation of these intelligent models is grounded in a set of well-established performance metrics, as outlined in Table 8. Accuracy remains the most reported metric, providing a general overview of classification performance. However, in clinical contexts where false positives or false negatives can carry significant consequences, additional metrics such as sensitivity, specificity, precision, and F1-score offer more nuanced insights. For instance, sensitivity is essential for assessing a model's ability to correctly detect collateral presence in ischemic regions, while specificity ensures accurate exclusion of non-collateral cases. More advanced metrics, such as the Kappa Score and Jaccard Index, are particularly useful in segmentation tasks and multi-class scenarios, offering insights into agreement and spatial overlap. Studies such as those by Ali et al. [111], Bağcılar et al. [105], and Wang et al. [28] reflect how these metrics can be used to evaluate not only accuracy but also clinical reliability and robustness across imbalanced datasets.

The importance of model selection and data strategy is further highlighted through performance comparisons, as summarized in Table 9. Wang et al. [28] demonstrated that using multi-image input rather than single-image input with ResNet34 significantly improved AUC from 0.85 to 0.89, reinforcing the value of temporal information in collateral evaluation. Raj et al. [27] showed that integrating AutoML with CNN in a

Table 8
The most often utilized DL performance measures in brain stroke Collateral Classification.

Performance Measure	Meaning	Also Referred To As	Mathematical Illustration
Accuracy	Correct classifications over total cases	Overall Success Rate	$\text{Accuracy} = \frac{TP+TN}{TP+TN+FP+FN}$
Sensitivity	Ability to correctly detect positive cases	Recall or True Positive Rate (TPR)	$\text{Sensitivity} = \frac{TP}{TP+FN}$
Specificity	Ability to correctly detect negative cases	True Negative Rate (TNR)	$\text{Specificity} = \frac{TN}{TN+FP}$
Precision	Correct positive predictions among all predicted positives	Positive Predictive Value (PPV)	$\text{Precision} = \frac{TP}{TP+FP}$
F1-Score	Harmonic mean of precision and recall	Balanced F-measure	$\text{F1} = 2 \times \frac{\text{Precision} \times \text{Sensitivity}}{\text{Precision}+\text{Sensitivity}}$
AUC-ROC	Overall ability to discriminate between classes	Area under ROC curve	ROC area between TPR and FPR
Kappa Score (KS)	Agreement measure between two raters beyond chance	Inter-rater Agreement	$\text{KS} = \frac{T_o - T_e}{1 - T_e}$ (where T_o = observed accuracy and T_e = expected accuracy)
Jaccard Index (JI)	Similarity between two sets	Intersection over Union (IoU)	$\text{JI} = \frac{TP}{TP+FP+FN}$
Mean Absolute Error (MAE)	Average absolute difference between prediction and ground truth	Absolute Error	$\text{MAE} = \frac{1}{n}\sum_{i=1}^{n}\lvert a_i - b_i \rvert$
Hausdorff Distance (HD)	Maximum boundary deviation between segmentation and ground truth	Hausdorff Metric	$\text{HD} = \max\left(\max_{x \in B_{GT}} d(x, B_{MS}), \max_{y \in B_{MS}} d(y, B_{GT})\right)$

multimodal setup improved accuracy from 91.17% to 94.11%, emphasizing the importance of combining structural and handcrafted features. Bağcılar et al. [105] validated the performance superiority of MPViT over ResNet and SVM, achieving the highest accuracy of 76.7%. Similarly, Ali et al. [111] found that VGG11 outperformed traditional classifiers in CBCT-based classification, demonstrating the strength of deep learning even in low-resolution modalities. Hokkinen et al. [59] further showed that 3D CNN models enhanced infarct core volume prediction accuracy over traditional CNN approaches, underscoring the importance of 3D spatial information in stroke imaging. These comparative results confirm that architectural innovations and multimodal strategies directly translate into measurable performance gains.

Explainability should be vessel-centric: saliency/Grad-CAM constrained to arterial territories (e.g., MCA) and overlays on CTA/CBCT improve clinician trust and error analysis. Data governance and model security (privacy, adversarial robustness) also warrant brief reporting in clinical AI studies. Despite rapid progress, several factors still hinder clinical translation. Cross-institution variability, limited large annotated cohorts, and the lack of explainable outputs remain major barriers. Prior studies, including Ali et al. [112], Aziz et al. [106], and Hokkinen et al. [59], emphasize the need for multicenter datasets, standardized imaging protocols, and visual explanation tools to support clinical acceptance. Making model outputs interpretable e.g., saliency maps and Grad-CAM constrained to vascular structures with concise decision rationales can strengthen trust in time-critical workflows. Overall, the literature shows a clear shift toward deep learning and hybrid intelligent systems that leverage advanced architectures, robust class-aware metrics, and multimodal inputs. To move from promising prototypes to safe bedside use, future work must prioritize generalizability, interpretability, and dataset scalability. The following section details the specific challenges and future scopes required to close this development-to-practice gap.

13. Challenges and future scopes in AI-based collateral classification

Deep learning has accelerated automated collateral grading on CTA, MRA, and CBCT, with convolutional models such as ResNet and VGG, as well as CNN-Transformer hybrids and AutoML fusion, reporting strong performance for distinguishing poor, intermediate, and good collateral status [28,105,27,112,111,59]. Translation into routine practice is limited by three linked areas: data resources, model development, and clinical implementation. Weaknesses at the data level often carry through to downstream stages and reduce reliability, fairness, and clinical utility.

From a data perspective, many cohorts are modest and single center, and external validation is still uncommon, particularly for CBCT acquired in the angiography suite, as summarised in Table 9. Differences in scanner vendor, reconstruction kernel, phase timing, and contrast bolus create domain shift that degrades generalisation across sites. Ground truth is also inconsistent: collateral scales such as Tan [23], Maas [24], and Miteff [25] are not aligned, inter observer agreement is uneven, and intermediate grades are often under represented, which adds label noise and class imbalance. CBCT further introduces motion, beam hardening, and restricted field of view, which can obscure delayed filling and complicate annotation.

Model development faces additional constraints. Headline metrics frequently focus on accuracy or AUC, while Table 8 indicates the need for per class sensitivity and specificity, precision-recall analysis, probability calibration, and uncertainty estimation to select safe operating thresholds and to allow abstention when confidence is low. Collateral grades are ordinal by design; treating them as flat categories discards useful structure and inflates errors on borderline cases. Spatiotemporal information from multiphase CTA is sometimes reduced to a single frame, which weakens the physiologic signal of delayed collateral recruitment. Robustness to protocol changes remains fragile, and practical engineering details such as low latency inference, stable DICOM or PACS integration, clear failure modes, and monitoring after deployment are not consistently reported.

Clinical implementation depends on trust, usability, and measurable patient benefit. Outputs that lack vascularly plausible visual explanations limit acceptance. Interfaces should deliver vessel-centred overlays and concise grade suggestions that fit emergency and angiography workflows without delaying intravenous thrombolysis or thrombectomy decisions. Prospective evidence that links model output to infarct growth, symptomatic haemorrhage, door to decision time, and 90-day modified Rankin Scale is limited, which restricts regulatory and institutional adoption. Sustainable use also requires operational safeguards, including drift detection, periodic recalibration, audit trails, and defined fallbacks for inadequate input quality.

Future progress is likely to arise from realistic data, appropriate learning formulations, rigorous evaluation, and seamless workflow integration rather than a single superior architecture. This review's specific contribution is to synthesise AI-driven collateral grading with an emphasis on in-suite CBCT and to harmonise reporting across recent studies by extracting modality, grading scale, validation scope, and metrics; we foreground workflow impact rather than algorithmic novelty, thereby complementing prior general stroke-AI surveys. Multicenter consortia that curate harmonised CTA and in-suit CBCT cohorts with

Table 9
Summary of AI-based collateral classification studies, including dataset characteristics, validation status, labeling, imaging modality, and performance gains.

Study / Model	Dataset (n) & Origin	Validation	Labeling	Imaging Modality	Performance Metrics (95% CI) / Gains
Wang et al. [28] (ResNet34, multi-image)	250 patients, China	Yes (external)	2 neuroradiologists, consensus	Multiphase CTA	AUC 0.89 (0.84–0.93), Acc. 87%; Gain: +0.04 AUC vs single-image
Raj et al. [27] (CNN + AutoML Fusion)	200 patients, India	Yes (cross-institution)	Guideline-based labeling	CTA + AutoML fusion	Acc. 94.1% (NR CI), AUC 0.91; Gain: +3% vs standalone CNN
Kuang et al. [105] (MPViT Transformer)	300 patients, multicenter (China)	Yes	3-radiologist consensus	CTA	Accuracy 76.7% (NR CI); Gain: higher than ResNet (73.6%) and SVM (67.7%)
Ali et al. [112] (ResNet18)	120 patients, Malaysia	No (internal only)	Single expert	CBCT	Acc. 65.9%, Sens. 77.6%, Spec. 52.6%, F1 = 0.70
Ali et al. [111] (VGG11)	85 patients, Malaysia	No	Single rater	CBCT	Acc. 58.3%, Sens. 75.5%, Spec. 44.1%; Outperformed DT, SVM, RF, k-NN
Hokkinen et al. [59] (3D CNN)	90 patients, Finland	Yes (internal CV only)	Consensus	CTA	Sens. 0.38, Spec. 0.89; Gain: improved infarct volume prediction vs 2D CNN

documented acquisition metadata and phase timing are fundamental. Where direct sharing is not feasible, federated learning and carefully validated synthetic augmentation can broaden diversity while preserving privacy. Ordinal or regression formulations that respect grading continuity, paired with spatiotemporal encoders such as 3D or 4D CNNs and CNN-Transformer hybrids, can better capture delayed filling dynamics. Domain generalisation and test time adaptation can improve resilience to protocol and scanner variation. Models should expose calibrated confidence and explicit abstention, and can gain clinical relevance by fusing imaging with covariates such as NIHSS, onset to scan time, vascular territory, and suspected aetiology. Evaluation should routinely report per class performance, area under the precision-recall curve for rare classes, calibration error, and decision curve analysis, together with external validation and stratified audits by sex, age, aetiology, territory, and time window. Prospective studies that measure workflow indicators and patient outcomes, with anatomy-aware explanations embedded directly in PACS and angiography consoles, are essential to close the gap from development to practice.

Within this context, Table 7 summarises prevailing model families and the balance between local structure and long range context; Table 8 Calibration (e.g., reliability plots, Brier score) and decision-curve analysis are rarely provided but are essential to quantify net clinical benefit; future studies should include these alongside discrimination metrics. Clarifies which metrics are most informative for safety critical and imbalanced tasks; and Table 9 contrasts datasets, labeling strategies, validation scope, and reported gains. Addressing the visible gaps in external validation and CBCT representation, together with ordinality and uncertainty aware modeling and transparent evaluation, offers a direct route to reliable and equitable deployment of AI for collateral classification in ischemic stroke.

Taken together, these observations point to four levers for safe, useful deployment data realism, task-appropriate learning, rigorous evaluation, and workflow integration. We translate them into the following practical priorities.

Future Directions. To advance AI-based collateral grading into clinical practice, future work should:

- Real-time assistant: Integrate with PACS/angiography consoles to render vessel-centred overlays and an ordinal grade (poor/intermediate/good) with calibrated confidence; support explicit abstention; keep clinicians in the loop without delaying intravenous thrombolysis (IVT) or endovascular thrombectomy (EVT).
- Multicentre data at scale: Conduct large, multicentre studies (especially CBCT) to improve generalisability and reduce single-site bias.
- Standardisation and sharing: Develop harmonised imaging protocols and open-access datasets to enable reproducibility and benchmarking.
- Interpretable, task-appropriate models: Use ordinal/spatiotemporal formulations and provide vascularly plausible explanations (e.g., saliency/Grad-CAM) to support decision-making.
- Multimodal fusion: Combine imaging (CTA/CBCT/MRI) with clinical covariates (e.g., NIHSS, onset-to-scan, vascular territory) to enhance diagnostic relevance and personalisation.

14. Conclusion

This review synthesised recent progress in AI-based collateral classification for ischemic stroke across CTA, MRA, and in-suite CBCT. Convolutional networks (e.g., ResNet, VGG) and hybrid designs that combine CNNs with Transformer backbones or multimodal fusion consistently achieve encouraging discrimination of poor, intermediate, and good collateral status. At the same time, translation to routine care remains constrained by heterogeneous data and labels, limited external validation particularly for CBCT uncalibrated outputs, and incomplete reporting of workflow integration. This review's specific contribution is to synthesise AI-driven collateral grading with an emphasis on in-suite CBCT and to harmonise reporting across recent studies by extracting modality, grading scale, validation scope, and metrics; we foreground workflow impact rather than algorithmic novelty, thereby complementing prior general stroke-AI surveys.

Across modalities, AI methods offer a path to faster and more reproducible collateral assessment than subjective visual grading. MRI provides superior soft-tissue contrast without ionising radiation, while CBCT shows intra-procedural promise; however, stroke-specific evidence for dose, cost, and workflow advantages of CBCT remains preliminary and should be interpreted cautiously.

Finally, the key obstacles and the most actionable next steps are clear. Principal bottlenecks include limited multicentre datasets (especially for CBCT), non-uniform labeling across collateral scales, domain shift from scanner/protocol/timing differences, and under-reported workflow engineering. The most direct path to clinical impact is to curate harmonised multicentre cohorts (or use federated learning where sharing is restricted); implement a real-time clinical assistant integrated with PACS/angiography consoles that renders vessel-centred overlays and an ordinal collateral assessment (poor/intermediate/good) with calibrated confidence, supports explicit abstention, and keeps clinicians in the loop without delaying IVT/EVT; model both the ordinal structure of collateral assessment and the temporal dynamics of multiphase imaging (e.g., 3D/4D encoders, CNN–Transformer hybrids); strengthen robustness via domain generalisation and test-time adaptation; expose calibrated probabilities with abstention on low-confidence cases; and

fuse imaging with clinical covariates (e.g., NIHSS, onset-to-scan time, vascular territory). Routine external validation, stratified audits, and prospective evaluations that track workflow KPIs (e.g., door-to-decision time) and patient outcomes (e.g., sICH, 90-day mRS) are essential for safe clinical implementation.

CRediT authorship contribution statement

Kazi Ashikur Rahman: Writing – review & editing, Writing – original draft, Software, Conceptualization. **Nur Hasanah Ali:** Writing – review & editing, Supervision, Project administration, Investigation, Funding acquisition. **Ahmad Sobri Muda:** Resources, Methodology, Funding acquisition, Data curation.

Declaration of competing interest

The authors declare that they have no known competing financial interests or personal relationships that could have appeared to influence the work reported in this paper.

Acknowledgement

The authors would like to thank Multimedia University (MMU) for supporting this research, as well as all contributors from the Fisabilillah R&D Grant Scheme (FRDGS) and the UTeM Kesidang Scholarship.

Data availability

No data was used for the research described in the article.

References

[1] V.L. Feigin, E. Nichols, G. Nguyen, et al., Global, regional, and national burden of stroke and its risk factors, 1990–2019: a systematic analysis for the global burden of disease study 2019, Lancet Neurol. 20 (10) (2021) 795–820.
[2] B.C. Campbell, P. Khatri, Stroke, Lancet 393 (10169) (2019) 169–182.
[3] C. Kong, Q. Feng, T. Yang, S. Qiao, X. Zhang, J. Pfeuffer, T. Han, Dynamically grading cerebral collateral circulation using 3d multi-inversion time arterial spin labeling in ischemic stroke: a comparison with digital subtraction angiography, Front. Neurol. 16 (2025) 1553216.
[4] D.S. Liebeskind, Collaterals in acute stroke: beyond the clot, Neuroimaging Clin. N. Am. 15 (3) (2005) 553–573.
[5] A.M.M. Boers, R. Sales Barros, I.G.H. Jansen, O.A. Berkhemer, L.F.M. Beenen, B.K. Menon, et al., Value of quantitative collateral scoring on ct angiography in patients with acute ischemic stroke, Am. J. Neuroradiol. 39 (2018) 1074–1082.
[6] L. Dissing-Olesen, S. Hong, B. Stevens, New brain lymphatic vessels drain old concepts, eBioMedicine 2 (8) (2015) 776–777.
[7] J. Emberson, K.R. Lees, P. Lyden, L. Blackwell, G. Albers, E. Bluhmki, et al., Effect of treatment delay, age, and stroke severity on the effects of intravenous thrombolysis with alteplase for acute ischaemic stroke: a meta-analysis of individual patient data from randomised trials, Lancet 384 (9958) (2014) 1929–1935.
[8] R. Bourcier, M. Goyal, D.S. Liebeskind, K.W. Muir, H. Desal, A.H. Siddiqui, et al., Association of time from stroke onset to groin puncture with quality of reperfusion after mechanical thrombectomy: a meta-analysis of individual patient data from 7 randomized clinical trials, JAMA Neurol. 76 (4) (2019) 405–411.
[9] G. Ma, Z. Yu, B. Jia, Y. Xian, Z. Miao, D. Mo, et al., Time to endovascular reperfusion and outcome in acute ischemic stroke: a nationwide prospective registry in China, Clin. Neuroradiol. 32 (4) (2022) 997–1009.
[10] T.J. Jie, M.S. Sayeed, Review on detecting pneumonia in deep learning, Int. J. Robot. Automat. Sci. 6 (1) (2024), eISSN: 2682-860X.
[11] N.A.A. Hamzah, W.M.D.W. Zaki, W.H.W.A. Halim, R. Mustafar, A.H. Saad, Evaluating the potential of retinal photography in chronic kidney disease detection: a review, PeerJ 12 (2024) e17786.
[12] World Health Organization, Stroke, cerebrovascular accident, Online, https://www.who.int/health-topics/stroke, 2022.
[13] C.W. Tsao, A.W. Aday, Z.I. Almarzooq, A. Alonso, A.Z. Beaton, M.S. Bittencourt, et al., Heart disease and stroke statistics—2023 update: a report from the American heart association, Circulation 147 (8) (2023) e93–e621.
[14] D. Lauer, J. Sulźenko, H. Malíková, I. Štětkářová, P. Widimský, Advances in endovascular thrombectomy for the treatment of acute ischemic stroke, Expert Rev. Neurother. 25 (6) (2025) 675–687.
[15] Centers for Disease Control and Prevention (CDC), "What is stroke?", 2024, Accessed: 2024-02-28.
[16] Centers for Disease Control and Prevention, About stroke, https://www.cdc.gov/stroke/about.htm, 2022. (Accessed 5 January 2022).
[17] C. Qin, S. Yang, Y.-H. Chu, H. Zhang, X.-W. Pang, L. Chen, L.-Q. Zhou, M. Chen, D.-S. Tian, W. Wang, Signaling pathways involved in ischemic stroke: molecular mechanisms and therapeutic interventions, Signal Transduct. Targeted Ther. 7 (2022) 215.
[18] J. Corliss, Understanding the different types of "brain attack", Harvard Health Publishing, reviewed by Christopher P. Cannon, MD, Apr. 2025.
[19] M. Zhang, Z. Long, P. Liu, Q. Qin, H. Yuan, Y. Cao, Y. Jia, X. Liu, Y. Yu, Y. Wu, B. Pei, J. Ye, M. Wang, F. Wang, Global burden and risk factors of stroke in young adults, 1990 to 2021: a systematic analysis of the global burden of disease study 2021, J. Am. Heart Assoc. 14 (3) (2025) e039387.
[20] D. Nguyen, S.W. Cheung, Y. Liu, M.T. Mackay, B. Stojanovski, M. Moodie, L. Gao, Examination of pediatric hemorrhagic stroke incidence: a systematic review and meta-analysis, J. Stroke Cerebrovasc. Dis. 34 (2025) 108344.
[21] D. Kuriakose, Z. Xiao, Pathophysiology and treatment of stroke: present status and future perspectives, Int. J. Mol. Sci. 21 (20) (2020).
[22] S.H. Hung, S.F. Kramer, E. Werden, J. Hall, G. Sharma, H. Asadi, V. Thijs, B.C. Campbell, A. Brodtmann, The association between pre-stroke physical activity and cerebral collateral circulation in acute ischaemic stroke, J. Clin. Neurosci. 137 (2025) 111314.
[23] P. Seners, G. Turc, I.L. Maier, W. Ben Hassen, J.-C. Baron, O. Naggara, C. Oppenheim, Clot burden score and collateral status improve prediction of early recanalization with intravenous thrombolysis, Stroke 52 (3) (2021) 940–947.
[24] H. Gensicke, F. Al-Ajlan, J. Fladt, B.C.V. Campbell, C.B.L.M. Majoie, S. Bracard, et al., Comparison of three scores of collateral status for their association with clinical outcome: the hermes collaboration, Stroke 53 (12) (2022) 3548–3556.
[25] F. Seker, J. Pfaff, M.E. Wolf, J. Sedlacik, G. Thomalla, J. Fiehler, N.D. Forkert, Impact of cta collateral status on clinical outcome in acute ischemic stroke, Clin. Neurol. Neursurg. 182 (2019) 105476.
[26] W.J. Powers, A.A. Rabinstein, T. Ackerson, O.M. Adeoye, N.C. Bambakidis, K. Becker, J. Biller, M. Brown, B.M. Demaerschalk, B. Hoh, E.C. Jauch, C.S. Kidwell, T.M. Leslie-Mazwi, B. Ovbiagele, P.A. Scott, K.N. Sheth, A.M. Southerland, D.V. Summers, D.L. Tirschwell, 2019 guidelines for the early management of patients with acute ischemic stroke: a guideline for healthcare professionals from the American heart association/American stroke association, Stroke 50 (12) (2019) e344–e418.
[27] R. Raj, D. Pruthviraja, A. Gupta, J. Mathew, S.K. Kannath, A. Prakash, J. Rajan, Multilevel multimodal framework for automatic collateral scoring in brain stroke, IEEE Access 12 (2024) 33730–33748.
[28] J. Wang, D. Tan, J. Liu, J. Wu, F. Huang, H. Xiong, T. Luo, S. Chen, Y. Li, Merging multiphase cta images and training them simultaneously with a deep learning algorithm could improve the efficacy of ai models for lateral circulation assessment in ischemic stroke, Diagnostics 12 (7) (2022) 1562.
[29] D. Tan, J. Liu, S. Chen, R. Yao, Y. Li, S. Zhu, L. Li, Automatic evaluation of multiphase cranial CTA collateral circulation based on a feature-fusion attention network, IEEE Trans. Nanobiosci. 22 (4) (2023) 789–799.
[30] E.W. Avery, A. Abou-Karam, S. Abi-Fadel, J. Behland, A. Mak, S.P. Haider, T. Zeevi, P.C. Sanelli, C.G. Filippi, A. Malhotra, C.C. Matouk, G.J. Falcone, N. Petersen, L.H. Sansing, K.N. Sheth, S. Payabvash, Radiomics-based prediction of collateral status from ct angiography of patients following a large vessel occlusion stroke, Diagnostics 14 (5) (2024) 485.
[31] K.M. Rexrode, T.E. Madsen, A.Y.X. Yu, C. Carcel, J.H. Lichtman, E.C. Miller, The impact of sex and gender on stroke, Circ. Res. 130 (4) (2022) 512–528.
[32] M. Goyal, B.K. Menon, W.H. van Zwam, D.W.J. Dippel, P.J. Mitchell, A.M. Demchuk, B.C.V. Campbell, C.B. Majoie, A. van der Lugt, M.A. de Miquel, G.A. Donnan, Y.B. Roos, A. Bonafe, R. Jahan, H.-C. Diener, L.A. van den Berg, E.I. Levy, O.A. Berkhemer, V.M. Pereira, J. Rempel, M. Millan, S.M. Davis, D. Roy, J. Thornton, L.S. Román, M. Ribó, D. Beumer, B. Stouch, S. Brown, D. Campbell, R.J. van Oostenbrugge, J.L. Saver, M.D. Hill, T.G. Jovin, Endovascular thrombectomy after large-vessel ischaemic stroke: a meta-analysis of individual patient data from five randomised trials, Lancet 394 (10200) (2019) 1729–1740.
[33] M.K. Georgakis, L. Parodi, S. Frerich, E. Mayerhofer, G. Tsivgoulis, J.P. Pirruccello, A. Slowik, T. Rundek, et al., Genetic architecture of stroke of undetermined source: overlap with known stroke etiologies and associations with modifiable risk factors, Ann. Neurol. 91 (5) (2022) 640–651.
[34] M.J. Reeves, C.D. Bushnell, G. Howard, S.M. Gargano, P.W. Duncan, G. Lynch, L.D. Lisabeth, Sex differences in stroke: epidemiology, clinical presentation, medical care, and outcomes, Lancet Neurol. 21 (11) (2022) 954–966.
[35] W.-D. Heiss, The ischemic penumbra: correlates in imaging and implications for treatment of ischemic stroke—the Johann Jacob Wepfer award 2020, Cerebrovasc. Dis. 50 (2) (2021) 175–184.
[36] S.M. Uniken Venema, J.W. Dankbaar, L. Wolff, A.C.G.M. van Es, M. Sprengers, A. van der Lugt, D.W.J. Dippel, H.B. van der Worp, M.C.R. investigators, Collateral status and recanalization after endovascular treatment for acute ischemic stroke, J. NeuroInterv. Surg. 15 (6) (2023) 531–538.
[37] Allina Health, Peripheral artery disease (pad), https://www.allinahealth.org/health-conditions-and-treatments/health-library/patient-education/helping-your-heart/types-of-heart-problems/peripheral-artery-disease, 2024. (Accessed 15 September 2025). Allina Health's Patient Education Department, reviewed by medical experts.

[38] B. Menon, B. O'Brien, A. Bivard, N. Spratt, A. Demchuk, F. Miteff, et al., Assessment of leptomeningeal collaterals using dynamic ct angiography in patients with acute ischemic stroke, J. Cereb. Blood Flow Metab. 33 (2013) 365–371.

[39] E.S. Gencer, E. Yilmaz, E.M. Arsava, R. Gocmen, M.A. Topcuoglu, Cerebral arterial collateral status, but not venous outflow profiles, modifies the effect of intravenous tissue plasminogen activator in acute ischemic stroke, Brain Circ. 11 (3) (2025) 123–130.

[40] J.Y. Young, P.W. Schaefer, Acute ischemic stroke imaging: a practical approach for diagnosis and triage, Int. J. Cardiovasc. Imag. 32 (1) (2016) 19–33.

[41] Q. Lu, H. Chen, J. Fu, X. Zheng, Y. Xu, Y. Pan, Automatic collateral quantification in acute ischemic stroke using u^2-net, Front. Neurol. 16 (2025) 1502382.

[42] S. Yoshimura, N. Sakai, H. Yamagami, K. Uchida, M. Beppu, K. Toyoda, Y. Matsumaru, A. Tsujino, J. Nakagawara, K. Minematsu, Y. Ito, J. Takahashi, M. Inoue, R. Kondo, K. Nishiyama, Y. Shiokawa, N. Ohara, K. Shigeta, T. Nishida, T. Takigawa, et al., Endovascular therapy for acute stroke with a large ischemic region, N. Engl. J. Med. 386 (14) (2022) 1303–1313.

[43] G.W. Albers, M. Goyal, et al., Thrombectomy for stroke at 6 to 16 hours with selection by perfusion imaging, N. Engl. J. Med. 378 (8) (2018) 708–718.

[44] K. Malhotra, N. Goyal, A.H. Katsanos, A. Filippatou, P. Mandava, J. Helenius, J.J. Chang, P. Khatri, E.A. Mistry, A.V. Alexandrov, G. Tsivgoulis, Association of statin pretreatment with collateral circulation and final infarct volume in acute ischemic stroke patients: a meta-analysis, Atherosclerosis 282 (2019) 75–79.

[45] I. Biose, J. Oremosu, S. Bhatnagar, et al., Promising cerebral blood flow enhancers in acute ischemic stroke, Transl. Stroke Res. 14 (2023) 863–889.

[46] J. Su, L. Wolff, A.C.G.M. van Es, W. van Zwam, C. Majoie, D.W.J. Dippel, A. van der Lugt, W.J. Niessen, T. van Walsum, Automatic collateral scoring from 3d cta images, IEEE Trans. Med. Imaging 39 (June 2020) 2190–2200.

[47] M.E. Amki, S. Wegener, Improving cerebral blood flow after arterial recanalization: a novel therapeutic strategy in stroke, Int. J. Mol. Sci. 18 (12) (2017) 2669.

[48] F. Ståhl, H. Almqvist, Å. Aspelin, et al., Stroke evaluation in the interventional suite using dual-layer detector cone-beam ct: a first-in-human prospective cohort study (the next generation x-ray imaging system trial), Clin. Neuroradiol. 34 (2024) 929–937.

[49] S. Lata, S. Mohanty, S. Vinay, A. Das, S. Das, P. Choudhury, Is cone beam computed tomography (cbct) a potential imaging tool in ent practice?: a cross-sectional survey among ent surgeons in the state of odisha, India, Indian J. Otolaryngol. Head Neck Surg. 70 (1) (2018) 130–136.

[50] C. Walter, J.C. Schmidt, C.A. Rinne, S. Mendes, K. Dula, A. Sculean, Cone beam computed tomography (cbct) for diagnosis and treatment planning in periodontology: systematic review update, Clin. Oral Investig. 24 (9) (2020) 2943–2958.

[51] E. Jing, H. Zhang, Z. Li, Y. Liu, Z. Ji, I. Ganchev, Ecg heartbeat classification based on an improved resnet-18 model, Comput. Math. Methods Med. 2021 (2021) 1–13.

[52] Y. Lei, T. Wang, S. Tian, X. Dong, A. Jani, D. Schuster, W. Curran, P. Patel, T. Liu, X. Yang, Male pelvic multi-organ segmentation aided by cbct-based synthetic mri, Phys. Med. Biol. 65 (3) (2020) 035003.

[53] N. Kabaliuk, A. Nejati, C. Loch, D. Schwass, J. Cater, M. Jermy, Strategies for segmenting the upper airway in cone-beam computed tomography (cbct) data, Open J. Med. Imag. 7 (4) (2017) 196–219.

[54] E. Venkatesh, S. Elluru, Cbct: basics and applications in dentistry, J. Istanbul Univ. Fac. Dent. 51 (2017) 102–121.

[55] I. Despotović, B. Goossens, W. Philips, Mri segmentation of the human brain: challenges, methods, and applications, Comput. Math. Methods Med. 2015 (2015) 1–23.

[56] K. Jeon, C. Lee, Y. Choi, S. Han, Comparison of the usefulness of cbct and mri in tmd patients according to clinical symptoms and age, Appl. Sci. 10 (10) (2020) 1–7.

[57] H. Hara, S. Yokoyama, S. Ohtomo, K. Takemoto, Y. Yoshida, S. Uchiyama, K. Toyoda, Comparative sensitivity of magnetic resonance imaging and computed tomography in detecting acute intracerebral hemorrhage, Stroke 52 (1) (2021) 94–102.

[58] V.D. Petroulia, J. Kaesmacher, E.I. Piechowiak, T. Dobrocky, S.M. Pilgram-Pastor, J. Gralla, F. Wagner, P. Mordasini, Evaluation of sine spin flat detector ct imaging compared with multidetector ct, J. NeuroInterv. Surg. 15 (3) (2022) 292–297.

[59] L. Hokkinen, T. Mäkelä, S. Savolainen, M. Kangasniemi, Computed tomography angiography-based deep learning method for treatment selection and infarct volume prediction in anterior cerebral circulation large vessel occlusion, Acta Radiol. Open 10 (November 29 2021) 20584601211060347.

[60] J. Chen, F. He, Y. Fu, J. Zhang, P. Chen, Z. Li, Anatomy, imaging, and hemodynamics of the cerebral venous system, Front. Neurosci. 16 (2022) 999134.

[61] A. Sinha, P. Stanwell, M.C. Killingsworth, S.M.M. Bhaskar, Prognostic accuracy and impact of cerebral collateral status on clinical and safety outcomes in acute ischemic stroke patients receiving reperfusion therapy: a systematic meta-analysis, Acta Radiol. 64 (2) (2023) 698–718.

[62] H. Kuang, W. Wan, Y. Wang, J. Wang, W. Qiu, Automated collateral scoring on ct angiography of patients with acute ischemic stroke using hybrid cnn and transformer network, Biomedicines MDPI 11 (2023) 243.

[63] G. Maguida, A. Shuaib, Collateral circulation in ischemic stroke: an updated review, J. Stroke 25 (2) (2023) 179–198.

[64] H.S. Markus, A. Pezzini, S. Debette, Cervical artery dissection and stroke: new insights into pathophysiology and treatment, J. Neurol. Neurosurg. Psychiatry 93 (9) (2022) 927–934.

[65] X. Xiang, Q. Xu, J. Zhang, P. Wu, Y. Wang, Z. Wang, W. Chen, Flair vascular hyperintensity and asymmetric prominent veins on swi as complementary markers of collateral circulation in acute ischemic stroke, Eur. J. Med. Res. 28 (1) (2023) 354.

[66] R. Padhi, A. Shanmugam, A. Maheswaran, V. Shethna, K.T. Kannan, P. Giridas, J. Maniyarasu, J. Dhanasekaran, Collateral score as a prognostic marker in acute anterior circulation stroke: a multiphase computed tomography angiography analysis, J. Neurosci. Rural Pract. 16 (2) (2025) 256–263.

[67] C.A. Potter, A.S. Vagal, M. Goyal, D.B. Nunez, T.M. Leslie-Mazwi, M.H. Lev, Ct for treatment selection in acute ischemic stroke: a code stroke primer, Radiographics 39 (6) (2019) 1717–1738.

[68] K. Li, H. Jiang, J. Yu, Y. Liu, L. Zhang, B. Ma, S. Zhu, Y. Qi, S. Li, Y. Huang, Y. Yang, X. Xia, L. Wen, Determinants of leptomeningeal collateral status in acute ischemic stroke: a systematic review and meta-analysis of observational studies, J. Am. Heart Assoc. 13 (23) (2024) e034170.

[69] X. Leng, H. Fang, T.W.H. Leung, D.S. Liebeskind, Collateral circulation in acute ischaemic stroke: assessment tools, clinical relevance, and therapeutic strategies, J. Neurol. Neurosurg. Psychiatry 93 (10) (2022) 1020–1030.

[70] Y. Peng, J. Liu, R. Yao, J. Wu, J. Li, L. Dai, S. Gu, Y. Yao, Y. Li, S. Chen, J. Wang, Deep learning-assisted diagnosis of large vessel occlusion in acute ischemic stroke based on four-dimensional computed tomography angiography, Front. Neurosci. 18 (2024) 1329718.

[71] R.A. Rava, S.E. Seymour, K.V. Snyder, M. Waqas, J.M. Davies, E.I. Levy, A.H. Siddiqui, C.N. Ionita, Automated collateral flow assessment in patients with acute ischemic stroke using computed tomography with artificial intelligence algorithms, World Neurosurg. 155 (2021) 748–760.

[72] J. Schmidhuber, Deep learning: past, present, and future, Neural Netw. 142 (2022) 100–127.

[73] D. Hendrycks, K. Gimpel, Gaussian error linear units (gelus), in: International Conference on Learning Representations (ICLR), 2022.

[74] J. Hu, L. Shen, G. Sun, Squeeze-and-Excitation Networks, vol. 42, IEEE, 2019, pp. 2011–2023.

[75] W. Rawat, Z. Wang, Deep convolutional neural networks for image classification: a comprehensive review, Neural Comput. 29 (9) (2017) 2352–2449.

[76] G. Litjens, T. Kooi, B.E. Bejnordi, A.A.A. Setio, F. Ciompi, M. Ghafoorian, J.A. Van Der Laak, B. Van Ginneken, C.I. Sánchez, A survey on deep learning in medical image analysis, Med. Image Anal. 42 (2017) 60–88.

[77] D. Shen, G. Wu, H.-I. Suk, Deep learning in medical image analysis, Annu. Rev. Biomed. Eng. 19 (2017) 221–248.

[78] A. Khan, A. Sohail, U. Zahoora, A.S. Qureshi, A Survey of the Recent Architectures of Deep Convolutional Neural Networks, vol. 53, 2020, pp. 5455–5516.

[79] H.-C. Shin, H.R. Roth, M. Gao, L. Lu, Z. Xu, I. Nogues, J. Yao, D. Mollura, R.M. Summers, Deep convolutional neural networks for computer-aided detection: Cnn architectures, dataset characteristics and transfer learning, IEEE Trans. Med. Imaging 35 (5) (2016) 1285–1298.

[80] M. Anthimopoulos, S. Christodoulidis, L. Ebner, A. Christe, S. Mougiakakou, Lung pattern classification for interstitial lung diseases using a deep convolutional neural network, IEEE Trans. Med. Imaging 35 (5) (2016) 1207–1216.

[81] K.A. Rahman, E.F. Shair, A.R. Abdullah, T.H. Lee, N.H. Nazmi, Deep learning classification of gait disorders in neurodegenerative diseases among older adults using resnet-50, Int. J. Adv. Comput. Sci. Appl. 15 (11) (2024).

[82] K. Simonyan, A. Zisserman, Very deep convolutional networks for large-scale image recognition, in: International Conference on Learning Representations (ICLR), 2015.

[83] R.B. Lincy, R. Gayathri, Off-line tamil handwritten character recognition based on convolutional neural network with vgg16 and vgg19 model, in: V.L.N. Komanapalli, N. Sivakumaran, S. Hampannavar (Eds.), Advances in Automation, Signal Processing, Instrumentation, and Control, Springer Nature Singapore, Singapore, 2021, pp. 1935–1945.

[84] S. Hussein, K. Cao, Q. Song, U. Bagci, Risk stratification of lung nodules using 3d cnn-based multi-task learning, in: International Conference on Information Processing in Medical Imaging, 2017, pp. 249–260.

[85] Y. Gao, X. Li, G. Wu, D. Shen, Fully convolutional networks for automated brain tumor segmentation, Med. Phys. 45 (7) (2018) 3048–3056.

[86] M.M.R. Islam, A.K. Asraf, S. Fong, Brain stroke lesion classification using deep learning and machine learning models, Health Inf. Sci. Syst. 8 (2020) 1–11.

[87] M. Zhou, H. Chen, L. Yu, Automatic detection and classification of acute ischemic stroke using deep residual networks, IEEE Access 10 (2022) 13577–13587.

[88] M. Mohri, A. Rostamizadeh, A. Talwalkar, Foundations of Machine Learning, 2nd ed., MIT Press, Cambridge, MA, 2018.

[89] C.M. Bishop, Pattern Recognition and Machine Learning, Springer, 2006.

[90] S. Albawi, T.A. Mohammed, S. Al-Zawi, Understanding of a Convolutional Neural Network, 2019, pp. 1–6.

[91] A.A. Mansour, A. Tilioua, M. Touzani, Bi-lstm, gru and 1d-cnn models for short-term photovoltaic panel efficiency forecasting case amorphous silicon grid-connected pv system, Results Eng. 21 (2024) 101886.

[92] A. S, J. Kathirvelan, Computer vision-based detection and classification of chemically ripened bananas and papayas at vendor site through deep learning ai models using real-time dataset, Results Eng. 26 (2025) 104730.

[93] Y. Zhu, F. Zhong, J. Gao, Y. Cao, X. Wang, Z. Jiang, Research on supraharmonic detection in renewable energy grid integration based on improved resnet18, Results Eng. 25 (2025) 104281.

[94] A. Myrzatay, L. Rzayeva, S. Bandini, I. Shaya, B. Saoud, I. Çolak, K. Kayisli, Predicting lan switch failures: an integrated approach with des and machine learning techniques (rf/lr/dt/svm), Results Eng. 23 (2024) 102356.

[95] A. Daza, J. Bobadilla, J.C. Herrera, A. Medina, N. Saboya, K. Zavaleta, S. Siguenas, Stacking ensemble based hyperparameters to diagnosing of heart disease: future works, Results Eng. 21 (2024) 101894.

[96] O. Maier, H. Handels, C.H. Sudre, et al., Machine learning for stroke lesion outcome prediction using multimodal mri: an international multicenter study, NeuroImage Clin. 34 (2022) 102944.

[97] Y.J. Lee, M.J. Joo, H.K. Yu, T.-J. Lee, H.J. Kim, Random forest regressor for predicting sensory texture of emotional designed packaging films, Results Eng. 25 (2025) 104147.

[98] R. Zhang, B. Jiang, Z. Li, Y. Li, L. Zhang, Random forest-based radiomics model predicts outcomes in acute ischemic stroke, Front. Neurol. 11 (2020) 681.

[99] H. Sundarasetty, S.K. Sahu, Tribological behavior of pla reinforced with boron nitride nanoparticles using taguchi and machine learning approaches, Results Eng. 26 (2025) 104772.

[100] A. Ali, M. Shahid, B. Raza, A. Khan, Application of knn and other machine learning methods in ischemic stroke outcome prediction, BMC Med. Inform. Decis. Mak. 21 (1) (2021) 173.

[101] R. Zhang, M. Li, X. Chen, et al., Decision tree model predicts outcomes in acute ischemic stroke patients after reperfusion therapy, Front. Neurol. 11 (2020) 824.

[102] K. Rahman, E. Shair, A. Abdullah, T. Lee, N. Ali, M. Zakaria, M.A. Betar, Classifying gait disorder in neurodegenerative disorders among older adults using machine learning, Int. J. Robot. Control Syst. 5 (2) (2025) 1083–1101.

[103] G. Tetteh, F. Navarro, R. Meier, J. Kaesmacher, J. Paetzold, J. Kirschke, C. Zimmer, R. Wiest, B. Menze, A deep learning approach to predict collateral flow in stroke patients using radiomic features from perfusion images, Front. Neurol. 14 (February 21 2023) 1039693.

[104] C. Tangwiriyasakul, P. Borges, G. Pombo, S. Moriconi, M.S. Elmalem, P. Wright, Y.-H. Mah, J. Rondina, R. Gray, S. Ourselin, P. Nachev, M.J. Cardoso, Deep generative computed perfusion-deficit mapping of ischaemic stroke, arXiv preprint, arXiv:2502.01334, 2025.

[105] Å. Bağcılar, et al., Automated lvo detection and collateral scoring on cta using a 3d self-configuring object-detection network: a multi-center study, Sci. Rep. 13 (1) (2023) 8834.

[106] A. Abd Aziz, L.I. Izhar, V.S. Asirvadam, T.B. Tang, A. Ajam, Z. Omar, S. Muda, Detection of collaterals from cone-beam ct images in stroke, Sensors 21 (23) (2021).

[107] M. Aktar, D. Tampieri, H. Rivaz, M. Kersten-Oertel, Y. Xiao, Automatic collateral circulation scoring in ischemic stroke using 4d ct angiography with low-rank and sparse matrix decomposition, Int. J. Comput. Assisted Radiol. Surg. 15 (September 2020) 1501–1511.

[108] O. Öman, T. Mäkelä, E. Salli, S. Savolainen, M. Kangasniemi, 3d convolutional neural networks applied to ct angiography in the detection of acute ischemic stroke, Eur. Radiol. Exp. 3 (1) (2019) 1–11.

[109] I.Q. Grunwald, et al., Collateral automation for triage in stroke: evaluating automated scoring of collaterals in acute stroke on computed tomography scans, Cerebrovasc. Dis. 47 (5–6) (2019) 217–222.

[110] A. Mittermeier, P. Reidler, M.P. Fabritius, B. Schachtner, P. Wesp, B. Ertl-Wagner, O. Dietrich, J. Ricke, L. Kellert, S. Tiedt, W.G. Kunz, M. Ingrisch, End-to-end deep learning approach for perfusion data: a proof-of-concept study to classify core volume in stroke ct, Diagnostics 12 (5) (2022) 1142.

[111] N.H. Ali, A.R. Abdullah, N.M. Saad, A.S. Muda, E.E.M. Noor, Automated classification of collateral circulation for ischemic stroke in cone-beam ct images using vgg11: a deep learning approach, BioMedInformatics 4 (3) (2024) 1692–1702.

[112] N.H. Ali, A.R. Abdullah, N.M. Saad, A.S. Muda, Collateral circulation classification based on cone beam computed tomography images using resnet18 convolutional neural network, Int. J. Adv. Comput. Sci. Appl. 14 (8) (2023) 179–185.

[113] D. Haussen, M. Bouslama, S. Dehkharghani, J. Grossberg, N. Bianchi, M. Bowen, et al., Automated ct perfusion prediction of large vessel acute stroke from intracranial atherosclerotic disease, Intervent. Neurol. 7 (2018) 334–340.

[114] J. Baek, B. Kim, J. Kim, D. Kim, J. Heo, H. Nam, et al., Utility of leptomeningeal collaterals in predicting intracranial atherosclerosis-related large vessel occlusion in endovascular treatment, J. Clin. Med. 9 (2020) 2784.

[115] D. Sun, X. Huo Raynald, N. Ma, F. Gao, D. Mo, et al., Prediction of intracranial atherosclerotic acute large vessel occlusion by severe hypoperfusion volume growth rate, J. Stroke Cerebrovasc. Dis. 31 (2022) 106799.

[116] A. Sinha, P. Stanwell, R. Beran, Z. Calic, M. Killingsworth, S. Bhaskar, Stroke aetiology and collateral status in acute ischemic stroke patients receiving reperfusion therapy—a meta-analysis, Neurol. Int. 13 (2021) 608–621.

[117] L. Román, B. Menon, J. Blasco, M. Hernández-Pérez, A. Dávalos, C. Majoie, et al., Imaging features and safety and efficacy of endovascular stroke treatment: a meta-analysis of individual patient-level data, Lancet Neurol. 17 (2018) 895–904.

[118] A. de Havenon, M. Mlynash, M. Kim-Tenser, M. Lansberg, T. Leslie-Mazwi, S. Christensen, et al., Results from defuse 3: good collaterals are associated with reduced ischemic core growth but not neurologic outcome, Stroke 50 (2019) 632–638.

[119] D. Liebeskind, H. Saber, B. Xiang, A. Jadhav, T. Jovin, D. Haussen, et al., Collateral circulation in thrombectomy for stroke after 6 to 24 hours in the dawn trial, Stroke 53 (2022) 742–748.

[120] J. Gerber, M. Petrova, P. Krukowski, M. Kuhn, A. Abramyuk, U. Bodechtel, et al., Collateral state and the effect of endovascular reperfusion therapy on clinical outcome in ischemic stroke patients, Brain Behav. 6 (2016) e00513.

[121] S. Schönenberger, J. Pfaff, L. Uhlmann, C. Klose, S. Nagel, P. Ringleb, et al., The impact of conscious sedation versus general anesthesia for stroke thrombectomy on the predictive value of collateral status: a post hoc analysis of the siesta trial, Am. J. Neuroradiol. 38 (2017) 1580–1585.

[122] F. Sallustio, C. Motta, S. Pizzuto, M. Diomedi, A. Giordano, V. D'Agostino, et al., Ct angiography-based collateral flow and time to reperfusion are strong predictors of outcome in endovascular treatment of patients with stroke, J. Neurointervent. Surg. 9 (2017) 940–943.

[123] J. Park, H. Kwak, G. Chung, S. Hwang, The prognostic value of ct-angiographic parameters after reperfusion therapy in acute ischemic stroke patients with internal carotid artery terminus occlusion: leptomeningeal collateral status and clot burden score, J. Stroke Cerebrovasc. Dis. 27 (2018) 2797–2803.

[124] A. Renú, C. Laredo, C. Montejo, Y. Zhao, S. Rudilosso, N. Macias, et al., Greater infarct growth limiting effect of mechanical thrombectomy in stroke patients with poor collaterals, J. Neurointervent. Surg. 11 (2019) 989–993.

[125] D. Weiss, B. Kraus, C. Rubbert, M. Kaschner, S. Jander, M. Gliem, et al., Systematic evaluation of computed tomography angiography collateral scores for estimation of long-term outcome after mechanical thrombectomy in acute ischaemic stroke, Neuroradiol. J. 32 (2019) 277–286.

[126] K. Al-Dasuqi, S. Payabvash, G. Torres-Flores, S. Strander, C. Nguyen, K. Peshwe, et al., Effects of collateral status on infarct distribution following endovascular therapy in large vessel occlusion stroke, Stroke 51 (2020) e193–e202.

[127] A. Sarraj, A. Hassan, J. Grotta, S. Blackburn, A. Day, M. Abraham, et al., Early infarct growth rate correlation with endovascular thrombectomy clinical outcomes: analysis from the select study, Stroke 52 (2021) 57–69.

[128] M. Anadani, S. Finitsis, F. Clarençon, S. Richard, G. Marnat, R. Bourcier, et al., Collateral status reperfusion and outcomes after endovascular therapy: insight from the endovascular treatment in ischemic stroke (etis) registry, J. Neurointervent. Surg. 14 (2022) 551–557.

[129] A. Ravindran, M. Killingsworth, S. Bhaskar, Cerebral collaterals in acute ischaemia: implications for acute ischaemic stroke patients receiving, 2021.

[130] S. Nannoni, C. Cereda, G. Sirimarco, D. Lambrou, D. Strambo, A. Eskandari, et al., Collaterals are a major determinant of the core but not the penumbra volume in acute ischemic stroke, Neuroradiology 61 (2019) 971–978.

[131] L. Lin, J. Yang, C. Chen, H. Tian, A. Bivard, N. Spratt, et al., Association of collateral status and ischemic core growth in patients with acute ischemic stroke, Neurology 96 (2021) e161–e170.

[132] D. Liebeskind, G. Cotsonis, J. Saver, M. Lynn, T. Turan, H. Cloft, et al., Collaterals dramatically alter stroke risk in intracranial atherosclerosis, Ann. Neurol. 69 (2011) 963–974.

[133] X. Leng, L. Lan, L. Liu, T. Leung, K. Wong, Good collateral circulation predicts favorable outcomes in intravenous thrombolysis: a systematic review and meta-analysis, Eur. J. Neurol. 23 (2016) 1738–1749.

[134] O. Zaidat, A. Yoo, P. Khatri, T. Tomsick, R. von Kummer, J. Saver, et al., Recommendations on angiographic revascularization grading standards for acute ischemic stroke: a consensus statement, Stroke 44 (2013) 2650–2663.

[135] S.J. Lee, J.M. Hong, J.S. Kim, J.S. Lee, Endovascular treatment for posterior circulation stroke: ways to maximize therapeutic efficacy, J. Stroke 24 (2022) 207–223.